

## **CHAPTER 3**

**Taking Natural Products to New Lengths:**

**Biosynthesis of Novel Carotenoid Families**

**Based on Unnatural Carbon Scaffolds**

## SUMMARY

In an extension of previous work in which biosynthetic routes to novel C<sub>45</sub> and C<sub>50</sub> carotenoid backbones were established in recombinant *E. coli*, we demonstrate the capacity of the C<sub>40</sub> carotenoid desaturase CrtI from *Erwinia uredovora* to accept and desaturate these unnatural substrates. Desaturation step number in the C<sub>45</sub> and C<sub>50</sub> pathways was not very specific, resulting in the production of at least 10 more C<sub>45</sub> and C<sub>50</sub> carotenoids. These compounds have never before been identified in nature or chemically synthesized. We also present evidence of the biosynthesis of a novel asymmetric C<sub>40</sub> backbone formed by condensation of farnesyl diphosphate (C<sub>15</sub>PP) with farnesylgeranyl diphosphate (C<sub>25</sub>PP), and the subsequent desaturation of this backbone by CrtI in an unusual manner. Under some conditions, we found that C<sub>40</sub>, C<sub>45</sub>, and C<sub>50</sub> carotenoid backbones synthesized in *E. coli* were oxidized by unknown chemical or enzymatic means, giving monohydroxylated backbone derivatives. Some of these hydroxylated species served as substrates for CrtI *in vitro*, leading to the production of still more novel carotenoids. The ability to supply CrtI with unnaturally large substrates *in vivo* has allowed us to show that this enzyme regulates its desaturation step number by sensing the end groups of its substrate, unlike certain fungal carotenoid desaturases whose step number is apparently determined by their particular multimeric state. Analysis of the different molecular mechanisms by which chemical diversity is generated and then propagated through our nascent pathways provides insight into how this occurs in nature and the selective pressures that have shaped the evolution of natural product biosynthetic enzymes and pathways.

## INTRODUCTION

Nature's wealth of small molecules has proven extremely useful to humankind as a source of medicines, fragrances, pigments, toxins, and other functional compounds. Many of these natural products have captivated scientists for decades with their highly complex structures and the elaborate biosynthetic routes by which they are generated. As products of evolution, the ~170,000 natural products characterized thus far (10) are a collective demonstration of the power of this simple algorithm to generate immense chemical diversity.

Inspired by the importance of natural products to health, culture, chemistry, and biology, we have been conducting our own evolution experiments with natural product biosynthetic pathways in the laboratory. By mimicking and accelerating some of the very same processes that drive natural evolution—mutation, gene transfer, and selection—we and others have shown that it is possible to evolve carotenoid biosynthetic pathways, a model system of choice, in new, unnatural directions in standard laboratory bacteria (3, 4, 31, 35, 42, 43, 45, 46, 48, 53, 54, 56). (See Chapter 1 for a detailed description of how biosynthetic pathways can be evolved in the laboratory.)

Carotenoids are ancient natural pigments that play vital roles in key biological processes such as photosynthesis, quenching of free radicals, and vision (57). The ~700 carotenoids identified in nature branch from only two major pathways. Over 95% of natural carotenoids are biosynthesized from the symmetric C<sub>40</sub> backbone phytoene, which is formed by condensation of two molecules of geranylgeranyl diphosphate (GGPP, C<sub>20</sub>PP) (**Figure 3.1**). The C<sub>40</sub> pathway, in addition to being the most diverse carotenoid pathway, is also the most widespread in nature, appearing in thousands of species of

bacteria, archaea, algae, fungi, and plants. A separate C<sub>30</sub> pathway that begins with the fusion of two molecules of farnesyl diphosphate (FPP, C<sub>15</sub>PP) (**Figure 3.1**) accounts for the remainder of natural carotenoid diversity. C<sub>30</sub> carotenoids are known in only a small group of bacteria such as *Staphylococcus*, *Streptococcus*, *Methylobacterium*, and *Heliobacterium* species (52). (See Chapter 1 for a more thorough description of the key enzymatic steps in carotenoid biosynthesis.)

Previously, our group reported the expansion of carotenoid biosynthesis with the generation of a novel C<sub>35</sub> carotenoid pathway in recombinant *E. coli* (53, 56). This unusual pathway, which begins with the heterocondensation of C<sub>15</sub>PP and C<sub>20</sub>PP to form an unnatural, asymmetric C<sub>35</sub> carotenoid backbone, was further diversified by coexpression of downstream carotenoid desaturases and cyclases, some of which were evolved in our laboratory for a particular function in the new pathway (see Chapter 1). This work led to the biosynthesis of at least ten new carotenoids never before identified in nature or chemically synthesized (53).

Our laboratory also reported the biosynthesis of novel C<sub>45</sub> and C<sub>50</sub> carotenoid backbones in recombinant *E. coli* expressing the Y81A mutant of the farnesyl diphosphate (C<sub>15</sub>PP) synthase from *Bacillus stearothermophilus*, BstFPS<sub>Y81A</sub> (37), and the F26A+W38A double mutant of the C<sub>30</sub> carotenoid synthase CrtM from *Staphylococcus aureus*, CrtM<sub>F26A,W38A</sub> (54). The first enzyme, BstFPS<sub>Y81A</sub>, synthesizes a mixture of C<sub>15</sub>PP, C<sub>20</sub>PP, and the very rare (see Discussion) farnesylgeranyl diphosphate (FGPP, C<sub>25</sub>PP). The next enzyme, CrtM<sub>F26A,W38A</sub>, has an expanded substrate and product range compared to wild-type CrtM, which can only synthesize C<sub>30</sub> and C<sub>35</sub> carotenoid backbones (53, 56). When BstFPS<sub>Y81A</sub> and CrtM<sub>F26A,W38A</sub> were coexpressed in *E. coli*, a

mixture of C<sub>35</sub>, C<sub>40</sub>, C<sub>45</sub>, and C<sub>50</sub> carotenoid backbones was produced (**Figure 3.1**, ref. (54)).

The above work did not investigate whether these unnaturally large C<sub>45</sub> and C<sub>50</sub> carotenoid backbones could be metabolized by carotenoid desaturases, leading to the introduction of an extended conjugated system (chromophore) and the resulting emergence of pigmentation in the C<sub>45</sub> and C<sub>50</sub> pathways. In addition, the lack of an asymmetric C<sub>40</sub> carotenoid backbone detected in extracts of *E. coli* cultures coexpressing BstFPS<sub>Y81A</sub> and CrtM<sub>F26A,W38A</sub> warranted further examination. From homo- or heterocondensation of the three precursors C<sub>15</sub>PP, C<sub>20</sub>PP, and C<sub>25</sub>PP, six different carotenoid backbones are theoretically possible: C<sub>30</sub>, C<sub>35</sub>, symmetric C<sub>40</sub> (phytoene, C<sub>20</sub>+C<sub>20</sub>), asymmetric C<sub>40</sub> (C<sub>15</sub>+C<sub>25</sub>), C<sub>45</sub>, and C<sub>50</sub> (see **Figure 3.1**). However, only one population of C<sub>40</sub> backbones was isolated, and it was assumed to be all phytoene (54). Since C<sub>15</sub>PP, C<sub>20</sub>PP, and C<sub>25</sub>PP are all present in the cells, as indicated by the biosynthesis of C<sub>35</sub>, C<sub>45</sub>, and C<sub>50</sub> carotenoid backbones (CrtM<sub>F26A,W38A</sub> has lost most of its C<sub>30</sub> synthesis capability (54)), it was unclear if asymmetric C<sub>40</sub> backbones were not discovered because they were not synthesized or because they could not be separated and distinguished from phytoene.

In this work, we demonstrate the remarkable substrate promiscuity of the carotenoid desaturase CrtI from *Erwinia uredovora* by showing that it can desaturate C<sub>45</sub> and C<sub>50</sub> backbones, leading to an array of pigmented C<sub>45</sub> and C<sub>50</sub> carotenoids. We reveal that the production of specific desaturation products and the absence of others provides insight into the mechanism by which CrtI regulates its desaturation step number. We also present evidence that the asymmetric C<sub>40</sub> carotenoid backbone is indeed synthesized by *E.*

*coli* expressing BstFPS<sub>Y81A</sub> and variants of CrtM, and that this unnatural backbone is processed by CrtI in an unusual manner. Finally, we show that large carotenoid backbones are further diversified in an unexpected manner by *in vivo* hydroxylation under certain conditions, and that some of these hydroxylated backbones can serve as alternative substrates for CrtI.

In addition to the potential technological uses of the new carotenoids we report herein, the biosynthetic routes by which they are synthesized provide a convenient laboratory model to study emergent metabolic pathways in nature. We show how analysis of the modes by which chemical diversity is propagated in the new carotenoid pathways can enhance our understanding of the mechanisms used by evolution to continually discover new small molecules.

## RESULTS

### **CrtI desaturates unnatural C<sub>45</sub>, C<sub>50</sub>, and asymmetric C<sub>40</sub> carotenoid backbones, resulting in the biosynthesis of numerous novel carotenoids**

*E. coli* XL1-Blue cells coexpressing BstFPS<sub>Y81A</sub>, a CrtM variant (either the F26L single mutant CrtM<sub>F26L</sub> or the F26A+W38A double mutant CrtM<sub>F26A,W38A</sub>), and wild-type CrtI from *E. uredoovora* synthesize at least ten novel desaturated carotenoids with C<sub>45</sub> or C<sub>50</sub> backbones. Structures **3**, **4**, **5**, **6**, **10**, **11a**, **11b**, **12a**, **12b/c**, and **13**, reported here for the first time, were identified by their high-performance liquid chromatography (HPLC) retention times, UV-visible spectra, and mass spectra (**Table 3.1**; **Figures 3.2**, **3.3**, and **3.6**). We also isolated an unusual 2-step desaturated C<sub>40</sub> carotenoid that is likely based on

an asymmetric C<sub>40</sub> backbone (structure **1**, see below). **Table 3.2** lists trivial and IUPAC-IUB semi-systematic names for the structures depicted in **Figures 3.2-3.4**.

*E. coli* cultures harboring the plasmid pUCmodII-*crtM*<sub>F26L</sub>-*crtI*-*bstFPS*<sub>Y81A</sub>, pUCmodII-*crtM*<sub>F26A,W38A</sub>-*crtI*-*bstFPS*<sub>Y81A</sub>, or the plasmids pUC18m-*bstFPS*<sub>Y81A</sub> and pAC-*crtM*<sub>F26A,W38A</sub>-*crtI* together synthesized mixtures of all of these novel desaturated carotenoids in different proportions and titers, depending on the expression plasmid(s). With all of these expression systems, we observed almost 100% conversion of the C<sub>45</sub> carotenoid backbone 16-isopentenylphytoene to desaturated C<sub>45</sub> carotenoids, while only about 25% of the C<sub>50</sub> backbone 16,16'-diisopentenylphytoene was converted to desaturated products (**Table 3.1**).

Whereas *E. uredoovora* CrtI primarily catalyzes four desaturation steps on phytoene (24, 33, 56), acts predominantly as a 4-step desaturase in a C<sub>30</sub> pathway (56), and performs 4-5 desaturation steps on C<sub>35</sub> carotenoids (53), the step number of CrtI is less well defined on C<sub>45</sub> and C<sub>50</sub> substrates. In the C<sub>45</sub> pathway, 2-, 3-, 5-, and 6-step products were isolated from *E. coli* cultures harboring the plasmids listed above; in the same cultures, 2-, 3-, 4-, and 6-step C<sub>50</sub> products were found. In both pathways, there was no clear majority product (**Table 3.1**). We refer to this imprecise desaturase behavior as “stuttering.” **Figures 3.2** and **3.3** depict the desaturation isomers of these C<sub>45</sub> and C<sub>50</sub> products whose biosynthesis is supported by the HPLC and MS data (see below).

In general, the UV-visible absorption spectra of the desaturated C<sub>45</sub> and C<sub>50</sub> carotenoids are hypsochromically shifted compared to those of C<sub>40</sub> carotenoids with the same number of conjugated double bonds (**Figure 3.6: 3** and **10** vs. ζ-carotene, **4** and **11a** vs. neurosporene, **12a** vs. lycopene; see **Figure 2.1** for C<sub>40</sub> structures). The spectra shown

in **Figure 3.6** are the most bathochromic of those measured before and after iodine-catalyzed photoisomerization, and most of these spectra exhibit *cis*-peaks (9) that are less or only slightly more intense than the corresponding C<sub>40</sub> standard (e.g., **11a** vs. neurosporene, **10** vs.  $\zeta$ -carotene). We therefore hypothesize that the hypsochromic shifts in the spectra of **3**, **4**, **10**, **11a**, and **12a** are not caused by a high proportion of *Z*- (*cis*) isomers, but rather by unfavorable interactions between these highly non-polar carotenoids and the much more polar, mostly-acetonitrile solvent.

Of special interest are C<sub>50</sub> carotenoids **11b** and **12b/c**. Compared with **11a**, the former has a spectrum that is hypsochromically shifted by 11 nm at the wavelength of maximum absorption,  $\lambda_{\max}$  (**Figure 3.6**), elutes slightly earlier in reverse-phase HPLC, is only one-tenth as abundant, and has an identical molecular ion at  $m/z = 674.2$  (**Table 3.1**). We believe that these properties are best explained by an unusual desaturation pattern in **11b** in which all three desaturation steps are on one side of the molecule (**Figure 3.3**) (we denote this as “3+0” desaturation). We are not aware of other carotenoids with a 3+0 desaturation pattern whose spectra we can compare with that of **11b**. However, 7,8,11,12-tetrahydrolycopene, an isomer of  $\zeta$ -carotene with a 2+0 desaturation pattern instead of the 1+1 pattern of  $\zeta$ -carotene (see **Figure 3.4**), has an absorption spectrum that is hypsochromically shifted by ~5 nm compared with that of  $\zeta$ -carotene (9, 14, 15, 51). Product **12b/c** has a spectrum that is hypsochromically shifted by 4 nm at  $\lambda_{\max}$  compared with that for **12a** (**Figure 3.6**), and it elutes slightly before **12a** in HPLC (**Table 3.1**). This species is only slightly less abundant than **12a** and has the same molecular ion at  $m/z = 672.3$  (**Table 3.1**). These properties suggest that **12b/c** is a 4-step desaturated C<sub>50</sub> carotenoid with a 3+1 desaturation pattern (**12b** in **Figure 3.3**). However, we cannot rule

out the possibility that **12b/c** has a 4+0 desaturation pattern (**12c**) or is a mixture of **12b** and **12c**, which is why we have designated its spectrum in **Figure 3.6** as “**12b/c**.”

Carotenoid **5** has the mass of a 5-step desaturated C<sub>45</sub> carotenoid, and its absorption spectrum corresponds closely with that of 3,4-didehydrolycopene, which has a 3+2 desaturation pattern (9, 25). There are two possible C<sub>45</sub> carotenoids with this desaturation pattern (**Figure 3.2**), and we could not distinguish by HPLC and MS analysis whether carotenoid **5** has specific structure **5a** or **5b**, or represents a mixture of the two. Similarly, it is not possible to confirm whether carotenoid **4** has precise structure **4a** or **4b** without synthetic standards or the use of advanced nuclear magnetic resonance techniques requiring up to tens of milligrams of sample (18, 32).

Spectra **6** and **13** are similar to the spectrum of 3,4,3',4'-tetrahydrolycopene with 6 desaturation steps in a 3+3 pattern (9). Spectrum **6** is slightly hypsochromically shifted compared to spectrum **13**; this effect is likely due to a significant proportion of *Z*-isomers in our sample of carotenoid **6**, evidenced by the greater relative absorbance of its *cis* peaks at 396 and 415 nm. Having no reason to believe that either **6** or **13** has an unusual desaturation pattern, we have depicted these structures in **Figures 3.2** and **3.3**, respectively, with symmetrical 3+3 desaturation.

Notably absent in all the extracts we analyzed of cultures expressing BstFPS<sub>Y81A</sub>, CrtM<sub>F26L</sub> or CrtM<sub>F26A,W38A</sub>, and CrtI were 4-step desaturated C<sub>45</sub> and 5-step desaturated C<sub>50</sub> carotenoids. We believe these observations, which may initially seem merely curious, can help to clarify the means by which this desaturase regulates its step number (see Discussion).

Carotenoid **1** was initially surprising to find in the above extracts. This molecule and  $\zeta$ -carotene have the same molecular ion at  $m/z = 540.2$  (**Table 3.1**), but compared with  $\zeta$ -carotene, carotenoid **1** has a slightly longer HPLC retention time (~19 vs. ~18 min) and a UV-visible spectrum that is hypsochromically shifted by 5 nm at  $\lambda_{\max}$  (**Figure 3.6**). Because both molecules are  $C_{40}$  carotenoids with equal masses and virtually identical polarities, this wavelength shift cannot be due to a change in solvent–analyte interaction. Rather, we believe the shift is due to a 2+0 desaturation pattern, and that carotenoid **1** is based on an asymmetric  $C_{40}$  ( $C_{15}+C_{25}$ ) backbone as shown in **Figure 3.4** (see Discussion).

#### ***E. coli* expressing only BstFPS<sub>Y81A</sub> and a variant of CrtM accumulate hydroxylated carotenoid backbones**

When *E. coli* XL1-Blue cells were transformed with the desaturase-free plasmids pUCmodII-*crtM*<sub>F26L</sub>-*bstFPS*<sub>Y81A</sub> or pUCmodII-*crtM*<sub>F26A,W38A</sub>-*bstFPS*<sub>Y81A</sub> and grown in liquid culture, they accumulated novel monohydroxylated  $C_{45}$  and  $C_{50}$  carotenoid backbones **7** and **14** as well as monohydroxylated  $C_{40}$  backbones, which may be novel depending on the location of the OH-group and whether the  $C_{40}$  backbone is symmetric or asymmetric (**Figures 3.5, 3.7** and **3.8**). The biosynthesis of these hydroxylated carotenoids was confirmed by MS and chemical derivatization (**Figure 3.9**), and their proportions relative to each other and the unmodified backbones were quite reproducible (**Figure 3.8**). On the other hand, similar XL1-Blue cultures harboring the plasmids pUC18m-*bstFPS*<sub>Y81A</sub> and pAC-*crtM*<sub>F26A,W38A</sub> did not produce hydroxylated backbones. Some possible reasons for this disparity are presented in the Discussion.

Although we could not identify the specific locations of the hydroxy groups by HPLC and MS analysis, we can exclude several possible regioisomers. The *in vitro* acetylation reactions with acetic anhydride described in Materials and Methods were positive for all the hydroxylated C<sub>40</sub>, C<sub>45</sub>, and C<sub>50</sub> backbones, with conversions above 90% in all cases. This indicates that the hydroxy groups are primary or secondary (19). Also, the propensity of the hydroxylated and acetylated carotenoids to lose water or acetate, respectively, in atmospheric pressure chemical ionization mass spectrometry (APCI-MS) (**Figure 3.9**) is evidence that the substituents are located in an allylic position (2). Finally, that some of these hydroxylated backbones are desaturated by CrtI *in vitro* (see below) suggests the OH group is located far from the center of the molecule. A hydroxy group located close to the center of a carotenoid backbone, which is where desaturases initiate their catalytic action, might interfere with the ability of a desaturase to process such a substrate.

Only one C<sub>40</sub> backbone fraction was seen in HPLC; likewise, hydroxylated C<sub>40</sub> backbones eluted as a single peak (**Figure 3.7**). Attempts to further separate these fractions using a linear gradient of acetonitrile:isopropanol (98:2 to 93:7 over 30 min.) also failed. However, because of the strong evidence that carotenoid **1** is based on the asymmetric C<sub>40</sub> carotenoid backbone 16-isopentenyl-4'-apophytoene, we nevertheless believe that the C<sub>40</sub> backbone fraction is a mixture of phytoene and 16-isopentenyl-4'-apophytoene, and that the C<sub>40</sub>-OH fraction may also be a mixture of hydroxylated versions of these backbones. Indeed, the subtle structural differences between symmetric and asymmetric backbones of the same length should have minimal effects on

chromatographic retention. Therefore, co-elution under our separation conditions would not be unexpected.

Cultures of *E. coli* strain HB101 carrying either plasmid pUCmodII-*crtM*<sub>F26L</sub>-*bstFPS*<sub>Y81A</sub> or pUCmodII-*crtM*<sub>F26A,W38A</sub>-*bstFPS*<sub>Y81A</sub> also synthesized hydroxylated C<sub>40</sub>, C<sub>45</sub>, and C<sub>50</sub> carotenoids, but in different relative proportions compared with the XL1-Blue cultures (data not shown). Surprisingly, significant proportions of acetylated C<sub>40</sub> and C<sub>45</sub> carotenoid backbones (~10 and ~19 mol% of total carotenoids, respectively) were detected in cultures of HB101(pUC18m-*bstFPS*<sub>Y81A</sub> + pAC-*crtM*<sub>F26A,W38A</sub>) in addition to smaller amounts of hydroxylated C<sub>40</sub> and C<sub>45</sub> carotenoid backbones (~2 and ~4 mol%, respectively). The *in vivo*-acetylated carotenoids behaved identically in HPLC and APCI-MS to their counterparts produced by *in vitro* derivatization of hydroxylated carotenoids with acetic anhydride. These acetylated backbones are probably formed by the reaction of hydroxylated carotenoids with acetyl-CoA, a process that is somehow promoted in HB101 cells carrying these plasmids.

### ***In vitro* desaturation experiments with CrtI**

In an effort to learn more about the substrate specificity of *E. uredo* CrtI and to potentially access new desaturated carotenoids, we carried out *in vitro* desaturation reactions in which an invariant amount of *E. coli* lysate containing CrtI was incubated with an individual carotenoid backbone (see Materials and Methods). These experiments, in which substrates dissolved in a small amount of acetone were added to cell lysate, yielded markedly different results compared with carotenoid desaturation in living cells, where carotenoid backbones already present in intact cell membranes are converted by membrane-bound desaturases. *E. uredo* CrtI converts all the available phytoene to

lycopene (and even tetrahydrolycopene) *in vivo*, leaving no intermediates (33, 56). *In vitro*, on the other hand, the enzyme converted an average of 19% of the phytoene to a mixture of mainly lycopene and intermediate products (**Table 3.3**). A similarly reduced *in vitro* efficiency on both native and non-native substrates was also seen for purified CrtI from *Rhodobacter capsulatus* and CrtN from *S. aureus* (39, 40), and appears to be a general feature of *in vitro* compared with *in vivo* carotenoid desaturation. This reduced efficiency is probably a consequence of suboptimal reaction conditions and substrate delivery *in vitro*. *In vivo*, carotenoids are sequestered together with desaturases in cell membranes, increasing the effective concentration of both enzyme and substrate. *In vitro*, proper association of carotenoid backbones and desaturases may be hampered. Additionally, inactivated desaturases are replenished with newly synthesized copies *in vivo* but not *in vitro*.

Of the intermediates detected and quantified by HPLC, 1-step phytofluene and 2-step  $\zeta$ -carotene were each present at approximately twice the level of 3-step neurosporene (**Table 3.3**, structures of these carotenoids are shown in **Figure 3.4**). This result qualitatively agrees with that of Fraser et al., who detected phytofluene and  $\zeta$ -carotene but not neurosporene in the product mixture when they supplied purified *E. uredo* CrtI with phytoene *in vitro* (24).

If we take the *in vitro* conversion statistics as a measure of the degree of compatibility between a substrate and CrtI, then comparing the fractional conversion of other backbones to the benchmark of ~19% conversion of phytoene can allow us to assess the substrate range of the enzyme, at least with respect to this relevant parameter. In this context, the C<sub>30</sub> diapophytoene is a much less favored substrate for CrtI, while the

C<sub>45</sub> backbone ranks between phytoene and diapophytoene in acceptability (**Table 3.3**). The C<sub>50</sub> backbone diisopentenylphytoene was not converted at all *in vitro*, reaffirming our *in vivo* results showing that a substantial proportion of this backbone synthesized in *E. coli* cells remained unmetabolized by CrtI. These results also further highlight the reduced efficiency that carotenoid desaturases display *in vitro*.

In addition to its much lower conversion *in vitro* (~5% vs. ~100% *in vivo*), the C<sub>45</sub> backbone also underwent fewer desaturation steps *in vitro*, with the terminal *in vitro* product being the 2-step carotenoid **3**. The predominant C<sub>45</sub> desaturation product *in vitro* was the 1-step carotenoid **2**, which was not detected at all *in vivo*. Therefore, the reduced step number displayed by CrtI *in vitro* on the C<sub>45</sub> backbone allowed access to a novel carotenoid that did not accumulate in cultured cells.

CrtI also desaturated hydroxylated C<sub>40</sub> and C<sub>45</sub> backbones, resulting in the production of (at least) two more new carotenoids, **8** and **9**. (The desaturated monohydroxy C<sub>40</sub> carotenoids OH-phytofluene, OH- $\zeta$ -carotene, OH-neurosporene, and OH-lycopene (see **Figure 3.5**) may also be novel, depending on the location of the hydroxy group.) Although the fungal carotenoid desaturase Al-1 from *Neurospora crassa* was reported to desaturate 1-OH-neurosporene and 1-OH-lycopene (25) and the 3-step desaturase from *R. capsulatus* was shown to efficiently accept 1,2-epoxyphytoene as a substrate (39), this is to our knowledge the first report of the desaturation of oxygenated carotenoids by a bacterial desaturase. Because the precise position of the hydroxy group in the C<sub>45</sub>-OH substrate **7** is unknown, we do not know the exact structures of products **8** and **9**. Accordingly, we have represented these carotenoids only by name in **Figure 3.5**. Interestingly, the average fractional conversion of the hydroxylated C<sub>45</sub> backbone was

almost three times that of the unmodified C<sub>45</sub> backbone, implying that the hydroxy group promotes desaturation *in vitro*. We are uncertain of the reason for this, but hypothesize that the increased polarity brought about by hydroxylation may enhance the ability of the substrate to be solubilized and therefore mix with the enzyme in the reaction medium. The hydroxy group on the C<sub>50</sub>-OH substrate **14**, however, did not appear to assist desaturation by CrtI *in vitro*. Neither it nor its unmodified counterpart was desaturated in these experiments. As with the C<sub>45</sub> backbone, the C<sub>45</sub>-OH backbone **7** was desaturated two steps *in vitro*, with a greater proportion of 2-step products accumulating in the latter reactions. The hydroxy group clearly does not interfere with the desaturation sequence of CrtI, at least up to the first two steps. We interpret this as evidence that the OH group is located distal to the center of the molecule.

Hydroxylated C<sub>40</sub> carotenoid backbones were also converted at a relatively high level (**Table 3.3**). It is not certain whether this substrate pool was a mixture of hydroxylated phytoene and hydroxylated 16-isopentenyl-4'-apophytoene, and if so, the proportion of each. However, judging by the relatively similar percentages of 1- to 4-step products in the phytoene and C<sub>40</sub>-OH desaturation experiments, we surmise that most of the C<sub>40</sub>-OH pool was hydroxylated phytoene. Therefore, we did not depict any hydroxylated asymmetric C<sub>40</sub> pathway products in **Figure 3.5**. We are not sure of the reason(s) for the increased proportion of 3-step products in the reactions with C<sub>40</sub>-OH backbones compared to phytoene. This may be somehow due to the hydroxy group on the substrate, but many other explanations are plausible. HPLC analysis of the 2-step desaturation products from the C<sub>40</sub>-OH reactions did not yield convincing evidence of a hydroxylated derivative of carotenoid **1**. This can be taken as additional evidence that

hydroxylated phytoene dominated the C<sub>40</sub>-OH backbone population. As with the C<sub>45</sub>-OH backbone, the hydroxy group on the C<sub>40</sub>-OH substrate does not inhibit the desaturation sequence of CrtI, as evidenced by the high proportion of 4-step desaturation products. We believe this result points to a terminal or near-terminal position of the OH group in the hydroxylated C<sub>40</sub> backbones.

### **Carotenoid biosynthesis in cultures expressing the C<sub>25</sub>PP synthase from *Aeropyrum pernix***

In an attempt to increase the proportion of C<sub>50</sub> carotenoids synthesized by our recombinant *E. coli*, we substituted BstFPS<sub>Y81A</sub> with the C<sub>25</sub>PP synthase from the thermophilic archaeon *Aeropyrum pernix*, ApFGS. Farnesylgeranyl diphosphate (FGPP, C<sub>25</sub>PP) is a very rare molecule in nature, and *apFGS* is the only natural C<sub>25</sub>PP synthase gene sequenced to date (50). We cloned *apFGS* from *A. pernix* genomic DNA and coexpressed it with *crtM*<sub>F26A,W38A</sub> on one plasmid as well as on separate plasmids.

ApFGS turned out to be disappointing as a C<sub>25</sub>PP synthase and mainly behaved as a C<sub>20</sub>PP synthase in our cells, as shown in **Figure 3.10**. When CrtM<sub>F26A,W38A</sub> is expressed alone in *E. coli* XL1-Blue(pUC18m-*crtM*<sub>F26A,W38A</sub>), only C<sub>30</sub> and C<sub>35</sub> carotenoids are synthesized (**Figure 3.10**, first data set). Expression of wild-type CrtM alone in *E. coli* results in almost exclusive production of C<sub>30</sub> diapophytoene (54), but CrtM<sub>F26A,W38A</sub> is a much poorer C<sub>30</sub> synthase and apparently a very effective scavenger of C<sub>20</sub>PP. Therefore, even though the endogenous level of C<sub>20</sub>PP is very low in *E. coli* and cannot support C<sub>40</sub> phytoene synthesis by the native C<sub>40</sub> synthase CrtB (see Chapter 2) or by CrtM<sub>F26A,W38A</sub> (**Figure 3.10**, first data set), the latter enzyme condenses abundant C<sub>15</sub>PP with much less abundant C<sub>20</sub>PP to such an extent that C<sub>30</sub> backbones outnumber C<sub>35</sub> backbones by only a

factor of 2 in XL1-Blue(pUC18m-*crtM*<sub>F26A,W38A</sub>). When ApFGS was coexpressed with *CrtM*<sub>F26A,W38A</sub> together on plasmid pUC18m-*apFGS-crtM*<sub>F26A,W38A</sub>, approximately equal proportions of C<sub>35</sub> and C<sub>40</sub> carotenoid backbones were synthesized (**Figure 3.10**, second data set). This indicates that ApFGS primarily synthesizes C<sub>20</sub>PP and also that a substantial amount of C<sub>15</sub>PP remains available for carotenoid biosynthesis in XL1-Blue(pUC18m-*apFGS-crtM*<sub>F26A,W38A</sub>) cells. When the same two genes were expressed on separate plasmids, XL1-Blue cultures harboring pUC18m-*apFGS* and pAC-*crtM*<sub>F26A,W38A</sub> synthesized the C<sub>40</sub> backbone phytoene almost exclusively, with traces of C<sub>45</sub> and C<sub>50</sub> backbones also being detected (**Figure 3.10**, fourth data set). This difference is most likely due to the differential copy number of the two plasmids. Being on a high-copy pUC-based plasmid, *apFGS* should be more highly expressed than *crtM*<sub>F26A,W38A</sub>, which is on a medium-copy pAC-based plasmid (both genes are under the control of identical *lac* promoter and operator sequences). The higher relative ApFGS level should therefore allow this enzyme to more completely consume the available C<sub>15</sub>PP before it can be incorporated into carotenoids by *CrtM*<sub>F26A,W38A</sub>. However, even when given this opportunity, ApFGS still releases primarily C<sub>20</sub>PP and only small amounts of C<sub>25</sub>PP.

ApFGS was shown to prefer C<sub>20</sub>PP as a substrate for synthesizing C<sub>25</sub>PP (50). Therefore, to see if increasing the supply of C<sub>20</sub>PP in the cells would result in a higher proportion of C<sub>45</sub> or C<sub>50</sub> carotenoids, we co-transformed XL1-Blue cells with pUC18m-*apFGS-crtM*<sub>F26A,W38A</sub> and pAC-*crtE* containing the C<sub>20</sub>PP synthase gene from *E. uredoovora*. This resulted in a ~3-fold increase in total carotenoids, and some C<sub>45</sub> backbones were detected, but phytoene represented the vast majority of the carotenoid

backbone pool in these cells (**Figure 3.10**, third data set). Evidently, ApFGS could not effectively compete with CrtM<sub>F26A,W38A</sub> for the additional C<sub>20</sub>PP supplied by CrtE.

*A. pernix* is a thermophilic organism, and ApFGS probably has an optimum temperature much higher than that at which *E. coli* cultures can be grown. However, cultivating ApFGS-expressing cultures at 37 °C instead of the usual 28 °C at which we grow our carotenogenic *E. coli* cultures did not increase the proportion of C<sub>45</sub> or C<sub>50</sub> carotenoids (data not shown). When CrtM<sub>F26A,W38A</sub> was coexpressed with ApFGS at 37 °C, almost no carotenoid backbones were synthesized. This may be due to compromised stability of this CrtM double mutant.

**The distribution of carotenoids synthesized by cells expressing BstFPS<sub>Y81A</sub> is strongly influenced by Idi overexpression and physiological state**

It is known that the biosynthesis of isoprenoids in *E. coli* is limited by the supply of the C<sub>5</sub>PP “starter unit” dimethylallyl diphosphate (DMAPP, structure shown in **Figure 1.4**), and that overexpression of isopentenyl diphosphate isomerase (Idi) can increase carotenoid titers by approximately an order of magnitude (59). In an effort to increase our carotenoid titers, we transformed XL1-Blue cells with plasmids pUC18m-*bstFPS<sub>Y81A</sub>-idi* (containing the *idi* gene from *E. coli*) and pAC-*crtM<sub>F26A,W38A</sub>*. After culturing these cells in TB medium, we found that Idi overexpression resulted in a ~10-fold increase in the quantity of carotenoids synthesized by the cells, but also dramatically shifted the distribution of carotenoid backbones toward production of phytoene (cf. first and second data sets in **Figure 3.11**). This result is likely due to alteration of the relative levels of isoprenyl diphosphate precursors of different lengths brought about by Idi overexpression (see Discussion).

In the course of our experiments involving coexpression of *bstFPS*<sub>Y81A</sub>, *crtM*<sub>F26L</sub> or *crtM*<sub>F26A,W38A</sub>, and *crtI*, we noticed that colonies expressing these genes from one or two plasmids reproducibly displayed a dramatically deeper red color than cell pellets from liquid cultures harboring the same plasmid(s). To investigate this further, we collected a sufficient quantity of the colonies (~0.5 g wet cells) to permit carotenoid extraction and HPLC analysis, and compared the carotenoid content of the colonies with that of the cell pellets. We discovered that the colonies primarily synthesized C<sub>40</sub> carotenoids and barely made any C<sub>45</sub> and C<sub>50</sub> products, while the liquid cultures inoculated by the very same colonies made substantial amounts of the larger carotenoids. This effect was also observed with no desaturase present (cf. first and third data sets in **Figure 3.11**) and occurred whether colonies were grown on LB- or TB-agar plates. Therefore, the dissimilar carotenoid distributions do not result from “defective” colonies, but rather, from differences in the physiology of *E. coli* colonies and liquid cultures. The strikingly similar shift toward an increased proportion of C<sub>40</sub> carotenoids at the expense of larger products caused by *Idi* overexpression and by cell growth in colonies is examined in more detail in the Discussion.

### **Attempted creation of a C<sub>60</sub> carotenoid biosynthetic pathway**

To ascertain whether our best C<sub>50</sub> carotenoid-producing *CrtM* variants or the C<sub>40</sub> synthase *CrtB* could also synthesize C<sub>60</sub> carotenoid backbones, we coexpressed the hexaprenyl diphosphate (C<sub>30</sub>PP) synthase *HexPS* from *Micrococcus luteus* (47) with *CrtM*<sub>F26L</sub>, *CrtM*<sub>F26A,W38A</sub>, or *CrtB* on plasmids pUC18m-*hexPS-crtM*<sub>F26L</sub>, pUC18m-*hexPS-crtM*<sub>F26A,W38A</sub>, and pUC18m-*hexPS-crtB*, respectively. However, we did not detect any carotenoids at all in cultures of XL1-Blue transformed with these plasmids. This

result indicates that HexPS is an active enzyme that consumes C<sub>15</sub>PP, since expression of *crtM*<sub>F26A,W38A</sub> alone on a pUC18m-based plasmid yields C<sub>30</sub> and C<sub>35</sub> carotenoids (**Figure 3.10**), and also that these synthases cannot synthesize C<sub>60</sub> carotenoids. Additional evidence also demonstrates that HexPS efficiently consumes C<sub>15</sub>PP and specifically synthesizes C<sub>30</sub>PP. XL1-Blue colonies harboring pUC18m-*crtM-crtN* are bright yellow due to the synthesis of large amounts of desaturated C<sub>30</sub> carotenoids (**Figure 3.12a**, panel 1). However, colonies transformed with pUC18m-*hexPS-crtM-crtN* are colorless, indicating considerable consumption of C<sub>15</sub>PP by HexPS (**Figure 3.12a**, panel 2). Coexpression of the C<sub>40</sub> carotenoid genes *CrtB* and *CrtI* further demonstrates that HexPS does not release C<sub>20</sub>PP. Whereas colonies harboring pUC18m-*crtE-crtB-crtI* are red-pink due to production of desaturated C<sub>40</sub> carotenoids beginning with the synthesis of C<sub>20</sub>PP by *CrtE* (**Figure 3.12a**, panel 3), colonies transformed with plasmid pUC18m-*hexPS-crtB-crtI* are colorless because *hexPS* does not supply *CrtB* with C<sub>20</sub>PP (**Figure 3.12a**, panel 4). Finally, *in vitro* experiments performed by Adam Hartwick show that when supplied with C<sub>15</sub>PP and isopentenyl diphosphate (IPP, structures shown in **Figures 3.1-3.5**), *CrtE* synthesizes the expected C<sub>20</sub>PP product (**Figure 3.12b**, lane 1), *BstFPS*<sub>Y81A</sub> synthesizes the expected C<sub>25</sub>PP product (**Figure 3.12b**, lane 2), and HexPS specifically synthesizes an even larger product (**Figure 3.12b**, lane 3). Similar experiments performed by Shimizu et al. confirmed with authentic standards that *M. luteus* HexPS indeed synthesizes primarily C<sub>30</sub>PP from C<sub>15</sub>PP and IPP (47).

No known carotenoid synthase, including our *CrtM* mutants, can convert C<sub>30</sub>PP to a C<sub>60</sub> carotenoid backbone. It may be possible to evolve one of these mutants or another carotenoid synthase in the laboratory for C<sub>60</sub> carotenoid synthesis. However, our results

showing poor conversion of the C<sub>50</sub> backbone to desaturated carotenoids by CrtI (**Tables 3.1 and 3.3**) and no conversion by the C<sub>30</sub> desaturase CrtN (data not shown) indicate that, should a biosynthetic route to C<sub>60</sub> backbones be established, desaturation of this substrate would be even less efficient by these enzymes. Therefore, no simple colorimetric assay exists for the screening of synthase variants in a directed evolution experiment aimed at evolving a C<sub>60</sub> carotenoid synthase.

## DISCUSSION

### **Determination of desaturation step number by *Erwinia* CrtI**

Elegant genetic complementation experiments with heterokaryons of the fungus *Phycomyces blakesleeanus* have provided convincing evidence for the existence of multienzyme complexes that function as assembly lines for carotenoid biosynthesis in that organism (5, 12, 16, 36). In these complexes, carotenoid substrates undergo stepwise chemical transformations as they are processed by one enzyme and then passed on to the next one in the complex, hence the analogy to an industrial assembly line. Therefore, phytoene undergoes four desaturation steps in *Phycomyces* because four desaturase subunits are present in that organism's carotenoid biosynthetic enzyme complexes (5). Carotenogenic enzyme complexes are believed to be widespread in other organisms as well, although there are many uncertainties regarding the factors that determine the extent of carotenoid desaturation (7).

Our results on the *in vivo* desaturation of the C<sub>45</sub> backbone isopentenylphytoene by *E. uredoovora* CrtI provide evidence against the idea that the number of subunits in a complex determines the desaturation step number. As mentioned, *E. uredoovora* CrtI is

primarily a 4-step desaturase in the symmetric C<sub>40</sub> pathway, converting phytoene to lycopene as the majority product (24, 33, 56). If the primary determinant of this 4-step product specificity were the association of CrtI subunits as tetramers, we should also expect primarily 4-step products with other carotenoid backbones as well, assuming these substrates are accepted and processed by the complex. However, not only is this not the case in the C<sub>45</sub> pathway, but 4-step C<sub>45</sub> products do not accumulate at all, even though 5- and 6-step C<sub>45</sub> carotenoids are detected (**Table 3.1, Figure 3.2**). Therefore, 4-step C<sub>45</sub> carotenoids are “skipped over” by CrtI *in vivo*, indicating a preference for synthesizing the higher step-number C<sub>45</sub> products **5** (5 steps, majority product) and **6** (6 steps, second-most abundant).

We believe this observation is related to two others. First, in the C<sub>50</sub> pathway, we observed no accumulation of 5-step products *in vivo* (**Table 3.1, Figure 3.3**), even though 6-step C<sub>50</sub> products were formed. Second, *in vitro* desaturation experiments with *E. uredovora* CrtI on phytoene have shown that the 3-step neurosporene is the least abundant intermediate, accumulating at low levels (**Table 3.3**) or not at all (24). (*In vivo*, the enzyme leaves behind no intermediates and even catalyzes six desaturation steps on phytoene (33, 56).)

These seemingly disparate phenomena are all connected by a common trait shared by neurosporene and the likeliest possible 4-step C<sub>45</sub> and 5-step C<sub>50</sub> products: all have one  $\psi$ -end and one dihydro- $\psi$ -end. This structural feature (see **Figure 1.8**) shared by all three disfavored products implies that *E. uredovora* CrtI has a strong propensity to avoid terminating its desaturation sequence at products with this combination of ends, regardless of the size of the carotenoid backbone substrate or the number of steps

required. Therefore, CrtI appears to regulate desaturation step number by sensing its substrate's end groups, with particular preference for carotenoids with one  $\psi$ - and one dihydro- $\psi$ -end, which are desaturated with high efficiency. The enzyme may accomplish this by having a higher affinity for substrates with these ends, but other strategies are possible. Whatever the specific mechanism, our results on C<sub>45</sub> and C<sub>50</sub> backbones clarify that the step number of this enzyme is significantly influenced by the size and end groups of its substrate. Thus, nature has apparently solved the problem of regulating carotenoid desaturation step number in at least two very different ways, as demonstrated by the distinct biochemical strategies employed by the phytoene desaturases of *E. uredoovora* and *P. blakesleeanus*.

These results also shed light on the functional plasticity displayed by bacterial carotenoid desaturases in directed evolution experiments aimed at altering desaturation step number (Chapter 1, refs. (46, 53, 58)). If a change in desaturation step number required a change in multimeric state, then converting a 4-step desaturase into a 6-step enzyme would require conversion of a tetrameric enzyme into a hexameric one. This would have to result from only a small number of mutations. While mutations can abolish the ability of a protein to form multimers, it seems much less plausible that the number of subunits in a complex could be so finely-tuned by minimal mutation. It is easier to envision how a desaturase's catalytic rate or tendency to synthesize products with particular end groups could be modified by mutation. Therefore, the relative ease and high frequency with which desaturation mutants have been discovered by directed evolution of bacterial desaturases are more easily rationalized in the light of altered specificity rather than multimeric state.

### Evidence of a novel asymmetric C<sub>40</sub> carotenoid biosynthetic pathway

We stated earlier that carotenoid **1** is likely the 2+0 desaturation product of an asymmetric C<sub>40</sub> (C<sub>15</sub>+C<sub>25</sub>) carotenoid backbone, as shown in **Figure 3.4**. Although **1** has the same mass and chromophore size as  $\zeta$ -carotene, it is unlikely that **1** is  $\zeta$ -carotene with the hypsochromic shift in its spectrum resulting from *Z*-isomerization. The spectrum of **1** (**Figure 3.6**) shows the hallmarks of a majority all-*E* sample population: the *cis* peaks at 286 and 295 are low ( $\sim 10\%$  of  $\lambda_{\max}$ ) and the ratio of the height of the longest-wavelength absorption band (419 nm) to the absorption at  $\lambda_{\max}$  (the so-called “III/II” ratio (9)) is 1.0. In fact, the spectrum shown for  $\zeta$ -carotene in **Figure 3.6** is that of a sample with more *Z*-isomer content than **1**. In that spectrum, III/II is only 0.83 (for all-*trans*  $\zeta$ -carotene, III/II is between 1.0 and 1.028 (14, 15)).

A 2+0 desaturation pattern also results in a hypsochromic shift of 5 nm, as shown by comparison of the spectrum of the 2+0 desaturation product of phytoene, 7,8,11,12-tetrahydrolycopene with that of  $\zeta$ -carotene, a 1+1 desaturated carotenoid (9, 14, 15, 51). However, although the absorption spectrum of 7,8,11,12-tetrahydrolycopene is strikingly similar to that of **1** (9, 14, 15, 51), it is also unlikely that carotenoid **1** is 7,8,11,12-tetrahydrolycopene, because *E. uredoovora* CrtI desaturates phytoene to lycopene via  $\zeta$ -carotene (**Table 3.3**, ref. (24)) and has not been shown to synthesize 7,8,11,12-tetrahydrolycopene. Furthermore, a 2-step desaturation product of phytoene like  $\zeta$ -carotene or 7,8,11,12-tetrahydrolycopene is not expected to accumulate in a culture expressing *E. uredoovora* CrtI. As mentioned previously, this enzyme desaturates all the available phytoene to lycopene and even 3,4,3',4'-tetrahydrolycopene *in vivo*, with no intermediates being detected. Indeed, in the same cultures in which **1** was found,

lycopene was also present and was usually at least twice as abundant; tetrahydrolycopene was also detected in smaller amounts (data not shown). Finally, the presence of a 2-step  $C_{40}$  carotenoid cannot be explained by a “phytoene overload” that overwhelms CrtI, for even in engineered *E. coli* that accumulate orders of magnitude more carotenoids than XL1-Blue, this desaturase is capable of efficiently converting the vastly increased phytoene supply to lycopene despite being expressed from a low-copy plasmid (20).

The most reasonable conclusion from the above evidence is that carotenoid **1** has an asymmetric  $C_{40}$  ( $C_{15}+C_{25}$ ) carbon backbone that has undergone two desaturation steps on its  $C_{15}$ -side. Although we were unable to separate the asymmetric  $C_{40}$  backbone 16-isopentenyl-4'-apophytoene from phytoene by HPLC of culture extracts of *E. coli* cultures expressing only BstFPS<sub>Y81A</sub> and a mutant of CrtM (**Figures 3.7** and **3.8**), it is reasonable to expect that the former backbone is made by these cultures, whose additional synthesis of  $C_{35}$ ,  $C_{45}$ , and  $C_{50}$  carotenoid backbones proves that both  $C_{15}$ PP and  $C_{25}$ PP are present in the cells. Furthermore, it is not surprising that CrtI would desaturate 16-isopentenyl-4'-apophytoene differently than phytoene. Although equal in size, the former is the most asymmetric of the six possible carotenoid backbones shown in **Figure 3.1**, and this likely affects the catalytic action of CrtI. When presented with the asymmetric  $C_{40}$  backbone, CrtI apparently catalyzes two desaturation steps on the  $C_{15}$ -side of the substrate (which is all that this side can accommodate) rather easily, but has trouble desaturating the  $C_{25}$ -side of the molecule; therefore, product **1** accumulates. (This scenario seems more probable than 2 steps on the  $C_{25}$ -side and none on the  $C_{15}$ -side since CrtI can desaturate the  $C_{30}$  ( $C_{15}+C_{15}$ ) backbone more efficiently than the  $C_{50}$  ( $C_{25}+C_{25}$ )

backbone (**Table 3.3**.) We are unsure why we did not detect any asymmetric C<sub>40</sub> pathway products with longer chromophores than **1**. Given that CrtI can desaturate C<sub>45</sub> and C<sub>50</sub> backbones, it is possible that some 4-6 step asymmetric C<sub>40</sub> pathway products were made but were not distinguished from symmetric C<sub>40</sub> carotenoids in our analysis, leaving only product **1** to stand out because of the lack of ζ-carotene produced. Because of this possibility, we could not quantify the relative proportions of symmetric and asymmetric C<sub>40</sub> carotenoids made in the cultures.

### **Potential utility of novel desaturated C<sub>45</sub> and C<sub>50</sub> carotenoids**

In this chapter, we report the biosynthesis of at least 14 new carotenoids based on unnatural carbon backbones. However, it remains to be seen whether any of these new products will prove technologically useful. Carotenoids are primarily sold for use as pigments, nutraceuticals, and as food and animal feed supplements (34). In some circumstances, a specific natural carotenoid is required, e.g., astaxanthin for salmon feed. However, in other current and envisioned applications such as antioxidant research and even microelectronics (11), “designer” molecules with specific properties not seen in natural carotenoids may prove extremely useful.

The chromophore of a carotenoid is the primary determinant of its color and chemical properties (8, 61, 63). C<sub>45</sub> and C<sub>50</sub> carotenoid backbones can in principle accommodate chromophores of 17 and 19 conjugated carbon-carbon double bonds, respectively, which is longer than the 15 possible on a C<sub>40</sub> backbone. Carotenoids with such large chromophores can absorb light at wavelengths above 600 nm, and their colors range from dark red to bluish purple (29, 35). Such carotenoids should be extremely reactive toward free radicals and could prove useful as potent antioxidants or colorants.

Although we did not generate carotenoids with more than 15 conjugated double bonds in this work, we have made progress toward this goal, and we believe that it will be possible to discover a desaturase in nature or to evolve one in the laboratory that can fully desaturate a C<sub>45</sub> or C<sub>50</sub> backbone. The insights we have gained about CrtI show that to evolve a 7- or 8-step desaturase will not require the discovery of extraordinarily rare mutants able to form heptamers or octamers, but merely variants with an altered preference for synthesizing carotenoids with fully desaturated end groups. Also, it may be possible to chemically desaturate 6-step C<sub>45</sub> and C<sub>50</sub> carotenoids even further (64), leading to carotenoids with chromophores of 17 or 19 conjugated double bonds.

Desaturated C<sub>45</sub> carotenoids **2**, **3**, **4**, **5**, and **6** (**Figure 3.2**) and desaturated C<sub>50</sub> carotenoids **10**, **11**, **12**, and **13** (**Figure 3.3**) reported in this work may be of interest for research purposes. Studies comparing the reactivity of these molecules toward free radicals in artificial lipid membranes could help researchers dissect the individual contributions of a carotenoid's chromophore, polarity, and end groups in determining this reactivity. For example, it is expected that the novel C<sub>45</sub> and C<sub>50</sub> carotenoids produced in this work should orient themselves deep within the hydrophobic core of a lipid bilayer, and such orientation effects are believed to strongly influence the *in vivo* antioxidant properties of a carotenoid (63).

Finally, it has been demonstrated that the presence of a single terminal hydroxy group in a carotenoid can dramatically improve its antioxidative properties (4). Therefore, the hydroxylation of carotenoid backbones we have observed in *E. coli* may be advantageous for the generation of monohydroxylated C<sub>45</sub> and C<sub>50</sub> carotenoids with desirable antioxidative abilities. Although we only observed hydroxylation of carotenoid

backbones *in vivo*, we showed that the hydroxylated C<sub>45</sub> backbone could be desaturated *in vitro*, generating 1- and 2-step monohydroxy C<sub>45</sub> structures **8** and **9**. Our results showing increased desaturation step number *in vivo* compared with *in vitro* (cf. **Tables 3.1** and **3.3**) point to a promising strategy for generating hydroxylated C<sub>45</sub> and C<sub>50</sub> carotenoids with longer chromophores: co-transform cells harboring pUCmodII-*crtM*<sub>F26L</sub>-*bstFPS*<sub>Y81A</sub> or pUCmodII-*crtM*<sub>F26A,W38A</sub>-*bstFPS*<sub>Y81A</sub> with another plasmid containing *crtI* under the control of a tightly-regulated promoter, and induce desaturase expression late in the culture. This approach would allow the cells to first accumulate monohydroxylated C<sub>45</sub> and C<sub>50</sub> backbones, which would then be desaturated *in vivo* upon desaturase expression. In nature, carotenoids are desaturated before they are hydroxylated. Therefore, it is interesting to note that this scheme could potentially produce highly desaturated monohydroxy C<sub>45</sub> and C<sub>50</sub> carotenoids with beneficial characteristics by an inverse biocatalytic route.

### **Origins of *in vivo*-hydroxylated carotenoids**

We remain uncertain of the mechanism by which the carotenoid backbones are hydroxylated *in vivo*. Krubasik et al. observed some hydroxylation of the C<sub>50</sub> flavuxanthin in recombinant *E. coli* cells (30) and C<sub>30</sub> carotenoids synthesized in *E. coli* have also been reported to be hydroxylated by unknown processes (31, 40). Lee et al. postulated that their C<sub>30</sub> diapocarotenoids were hydroxylated by free peroxy radicals present in *E. coli* membranes (31). Like us (56), they did not observe hydroxylation of C<sub>40</sub> carotenoids in *E. coli*. Albrecht et al. reported a significant amount of epoxidation and hydroxylation of phytoene in cells of the green algae *Scenedesmus acutus* whose phytoene desaturase was inhibited by the herbicide norflurazon (2). Their report

suggested that the origins of the oxygenated phytoene derivatives might be enzymatic, but the oxidation was later attributed to reaction with free radicals (G. Sandmann, personal communication).

As mentioned, XL1-Blue cultures harboring the plasmids pUC18m-*bstFPS*<sub>Y81A</sub> and pAC-*crtM*<sub>F26A,W38A</sub> produced no hydroxylated backbones (**Figure 3.8**). These cultures also produced fewer total carotenoids than the single-plasmid cultures (see **Figure 3.8** caption). This expression vector-dependency of carotenoid backbone hydroxylation suggests that *E. coli* cells selectively induce carotenoid oxidation only under certain conditions. Perhaps the lack of a *lac* operator in the pUCmodII-based plasmids and the resulting high-level constitutive expression of the carotenoid biosynthetic genes therein elicits this activation in *E. coli*. Plasmids pUC18m-*bstFPS*<sub>Y81A</sub> and pAC-*crtM*<sub>F26A,W38A</sub> have their carotenogenic genes under the control of a *lac* promoter and operator, which should limit gene expression somewhat and possibly avoid the same response in the cells. Alternatively, the induction of carotenoid backbone hydroxylation might be triggered when the quantity of large carotenoid backbones in the cell membrane reaches a critical threshold. It is possible that, in response to excessive loss of membrane fluidity brought on by the accumulation of highly nonpolar C<sub>45</sub> and C<sub>50</sub> carotenoid backbones, the cells up-regulate an oxidase or radical-producing enzyme that helps to rectify this problem by effecting hydroxylation of the offending molecules, thereby increasing their polarity. Similarly, accumulation of these carotenoids may disrupt a portion of the respiratory electron transport chain only when their concentration reaches a certain value, causing electron leakage and the production of reactive oxygen species. These hypotheses, although attractive, are only weakly supported by the fact that the carotenoid titer of

XL1-Blue(pUCmodII-*crtM*<sub>F26L</sub>-*bstFPS*<sub>Y81A</sub>) is a mere ~50% higher than that of XL1-Blue(pUC18m-*bstFPS*<sub>Y81A</sub> + pAC-*crtM*<sub>F26A,W38A</sub>) (see **Figure 3.8** caption).

Coexpressing CrtI along with BstFPS<sub>Y81A</sub> and either CrtM<sub>F26L</sub> or CrtM<sub>F26A,W38A</sub> abolished almost all carotenoid backbone hydroxylation in the cells even though C<sub>50</sub> backbones were quite abundant and accounted for ~50 mol% of total carotenoids. In these cultures, hydroxylated C<sub>50</sub> backbones represented only ~1 mol% of the carotenoid pool. A possible reason for this is that free radicals preferentially react with and are quenched by desaturated carotenoids, whose extended chromophores are much more reactive toward radical species compared with undesaturated carotenoid backbones (17, 57, 61, 63).

The above evidence points to radical oxygen species as the culprit in carotenoid backbone hydroxylation. However, the sharp, single HPLC peaks in **Figure 3.7** suggest a high degree of regiospecificity of the hydroxylation reactions and therefore direct enzymatic oxidation. If multiple positions of these backbones were hydroxylated, as might be expected if the mechanism were chemical oxidation by reactive oxygen species, we should observe multiple clustered HPLC peaks, each corresponding to a different positional isomer of a hydroxylated backbone. (Different hydroxylated regioisomers should have much more distinct chromatographic properties than symmetric or asymmetric versions of a C<sub>40</sub> backbone.) Indeed, an HPLC chromatogram showing multiple clustered peaks corresponding to different regioisomers of hydroxylated phytoene was generated by Albrecht et al. under chromatographic conditions similar to ours (2). On the other hand, the apparent regiospecific hydroxylation of our carotenoid backbones may result from their orientation in the cell membranes. For example, it is

possible that the backbones are positioned in such a manner that one end of the molecule protrudes from the membrane and consequently becomes prone to free-radical oxidation.

Clearly, additional research will be required to uncover the origins of carotenoid backbone hydroxylation in *E. coli*. It would probably be simplest to first conduct *in vitro* investigations of the reactions of the various backbones with free radicals generated *in situ* in a manner similar to that described by Woodall et al. (61). If hydroxylated products from these reactions closely match those we have reported, this result would support the hypothesis that similar radical reactions are responsible for carotenoid hydroxylation *in vivo*. On the other hand, if the products are not a close match, and especially if multiple clustered peaks are observed under the same HPLC conditions, then the possibility of enzymatic hydroxylation might warrant further investigation. We anticipate, however, that the search for an enzyme responsible for these transformations would be a very challenging experiment. For one, screening of genomic libraries would be very difficult since this could not be done in *E. coli*, and selection of another host organism does not seem straightforward. However, the fact that carotenoid hydroxylation only occurs with certain strain and plasmid combinations suggests that microarray identification of differentially expressed genes might be fruitful.

### **Properties of nascent biosynthetic pathways—lessons for biology and metabolic pathway engineering**

In addition to producing several novel carotenoids based on unnatural carbon scaffolds, this work has allowed us to investigate the precise biomolecular phenomena that resulted in the evolution of three novel biosynthetic pathways to carotenoid pigments. In this section, we analyze the specific mechanisms by which novel chemical diversity

was generated and propagated along these new pathways by their constituent enzymes. We then discuss key properties our pathways likely share with nascent biosynthetic pathways in general.

The Y81A amino acid substitution in BstFPS<sub>Y81A</sub> dramatically broadens the specificity of this enzyme, converting it from a strict C<sub>15</sub>PP synthase into an enzyme that synthesizes a mixture of C<sub>15</sub>PP, C<sub>20</sub>PP, and C<sub>25</sub>PP. This mutation has been studied in detail, and its effect on the enzyme's product range has been shown to result from an enlarged product elongation pocket (37). The Y81A mutation transforms BstFPS into a "statistical" biocatalyst. Although capable of synthesizing products up to C<sub>25</sub>PP by catalyzing two additional condensations of IPP with the growing prenyl chain, BstFPS<sub>Y81A</sub> also releases intermediates C<sub>15</sub>PP and C<sub>20</sub>PP; hence a distribution of prenyl diphosphate products with 3, 4, and 5 isoprene units is generated. The diversity of this product mixture is then amplified by the next enzyme in the pathway, a mutant of the *S. aureus* C<sub>30</sub> carotenoid synthase CrtM.

In Chapter 1, we discussed the molecular effects of mutations at F26 and W38 in CrtM. A homology model with human squalene synthase allowed us to map these residues to the site of the second half-reaction and led us to propose that their substitution with smaller amino acids increases the size of the cavity where cyclopropyl intermediates are rearranged into carotenoid backbones. From this analysis, we conjectured that wild-type CrtM could accept C<sub>20</sub>PP and even C<sub>25</sub>PP as substrates and form cyclopropyl intermediates from these precursors, but cannot rearrange intermediates larger than C<sub>35</sub> into carotenoid backbones. When additional space is created in the rearrangement pocket by replacement of F26 and/or W38 with smaller amino acids, conversion of the larger

intermediates becomes possible, resulting in the synthesis of carotenoid backbones up to C<sub>50</sub>. Like BstFPS<sub>Y81A</sub>, these CrtM mutants have lost much of their capacity to regulate the size of their products. When coexpressed with BstFPS<sub>Y81A</sub> *in vivo*, the CrtM mutants condense every possible pairwise combination among C<sub>15</sub>PP, C<sub>20</sub>PP, and C<sub>25</sub>PP except, intriguingly, the wild-type's combination of two molecules of C<sub>15</sub>PP (a consequence of the relatively low C<sub>15</sub>PP concentration combined with the intrinsically poor ability of the CrtM variants to make C<sub>30</sub> carotenoids). The result is a mixture of C<sub>35</sub>, symmetric (C<sub>20</sub>+C<sub>20</sub>), and asymmetric (C<sub>15</sub>+C<sub>25</sub>) C<sub>40</sub>, C<sub>45</sub>, and C<sub>50</sub> carotenoid backbone products.

The desaturase CrtI then further diversifies the five carotenoid backbones generated by the two previous enzymes. CrtI possesses no mutations, but its inherent promiscuity allows it to accept all of the above backbones to some degree. In the C<sub>45</sub> and C<sub>50</sub> pathways, the step number of CrtI is not very well defined (except for the absence of certain products discussed above), and there was no clear majority desaturation product in these pathways *in vivo* (**Table 3.1**). Therefore, the stuttering action of CrtI on the C<sub>45</sub> and C<sub>50</sub> backbones is the primary catalytic basis for the branching of these new pathways. As previously discussed, CrtI very efficiently catalyzes four desaturation steps on its native substrate phytoene *in vivo*. Under less optimal *in vitro* conditions, however, substantial stuttering occurs with the same substrate, and all possible intermediates in the desaturation sequence are detected (**Table 3.3**). In the more favorable milieu of a cell membrane, however, CrtI can still be made to stutter when presented with unnaturally large carotenoid backbones. We do not know the exact reason for this, but expect it is due to a decreased catalytic efficiency on these substrates. CrtI also produces carotenoids with unusual desaturation patterns like **1**, **11b**, and **12b/c** (**Figures 3.3**, **3.4**, and **3.6**;

**Table 3.1**), indicating that unnaturally large or asymmetric substrates can cause the enzyme to become slightly “confused” and carry out non-standard desaturation sequences. It is interesting that the unusual catalytic behavior that can result when an iterative enzyme is challenged with a new substrate can serve as a diversity-generating mechanism in the evolution of novel biosynthetic pathways.

This work demonstrates the rapid product diversification that is possible when biosynthetic pathways are constructed from multiple broad-specificity enzymes arranged consecutively. Such arrangements were likely very common in the early evolution of metabolism. The widely accepted “patchwork” model states that the first metabolic pathways were assembled from promiscuous enzymes whose specificities were then narrowed by natural selection, yielding the relatively specific pathways we see in nature today, especially in so-called primary metabolism (27, 41, 62). Our laboratory-generated carotenoid biosynthetic pathways also probably share key features with recently evolved metabolic pathways in nature. Most notably, a lack of overall pathway specificity characterized by the generation of multiple products is a trait likely common to nascent pathways created both in nature and in the laboratory. Directed evolution experiments on a wide range of enzymes demonstrate that it is rare for enzymes to completely shift their substrate or product specificity after accumulating only a small number (1-2) of mutations. Rather, mutants with broadened specificity are the norm, even if the selection pressure of the experiment requires only one particular reaction to be catalyzed (1). In nature, enzymes that have recently evolved the ability to accept non-native substrates such as man-made antibiotics also tend to have broadened rather than shifted specificities, hence the emergence of so-called “extended-spectrum” beta-lactamases (13). Therefore,

new biosynthetic pathways (or pathway branches) that have emerged in nature as a result of enzyme mutation probably possess low product specificity, similar to our nascent carotenoid pathways, especially when multiple enzymes have been mutated. In many if not most cases, it remains to be seen how many more mutations would be required and how strong the selection pressures would have to be in order to convert newly emerged pathways into mature ones capable of specifically synthesizing a particular complex end product.

Analysis of the means by which our novel carotenoid pathways have emerged also helps to clarify some aspects of a popular theory about the evolution of natural product biosynthetic pathways. The “screening hypothesis” put forth by Jones and Finn argues that natural product pathways have evolved under selection for particular traits, such as pathway branching and enzymatic promiscuity, because such traits promote the production and retention of product diversity at minimal cost (Chapter 1, refs. (21-23, 28)). However, our highly branched carotenoid pathways comprising laboratory-evolved promiscuous enzymes emerged despite a lack of selection for these properties. In no instance was selection for a diverse array of products applied in the laboratory evolution and subsequent site-directed mutagenesis experiments that resulted in the discovery of mutants BstFPS<sub>Y81A</sub>, CrtM<sub>F26L</sub>, and CrtM<sub>F26A,W38A</sub> (37, 38, 54-56). Yet, in all these cases, as is typical in directed evolution (see previous paragraph), enzyme variants with broadened specificity were obtained. This implies that traits such as enzyme promiscuity and the types of pathway branching to which it can lead do not require selection to arise or be maintained, but merely represent the default state of enzymes and metabolic pathways in the absence of strong and sustained selective pressure to be highly specific.

Therefore, we believe that the low specificity of many natural product biosynthetic enzymes and pathways is not the outcome of positive selection for promiscuity, but is more aptly attributed to genetic drift caused by weak selection pressure for narrow specificity, or to selection pressures that change rapidly and hence do not allow sufficient evolutionary time for any particular narrow specificity to fully develop.

### **Challenges for achieving new pathway specificity**

In the Results section, we described several unsuccessful experiments aimed at establishing more specific pathways in *E. coli* to particular novel-backboned carotenoids. For example, it should be possible to increase the proportion of C<sub>50</sub> carotenoids by increasing the proportion of C<sub>25</sub>PP relative to C<sub>15</sub>PP and C<sub>20</sub>PP. If it were possible to drive the fraction of C<sub>25</sub>PP to nearly 100%, it would not be necessary to further evolve a carotenoid synthase for increased C<sub>50</sub> product specificity because only one substrate would be available and therefore only the C<sub>50</sub> carotenoid backbone would be possible. As mentioned earlier, C<sub>25</sub>PP is a very rare molecule in nature. Its only biological role found to date is as a precursor for the C<sub>25</sub>-C<sub>25</sub> and C<sub>20</sub>-C<sub>25</sub> ether-linked membrane lipids of some archaea such as *Aeropyrum pernix* and *Natronomonas pharaonis* (6, 49, 50). C<sub>25</sub>PP synthase enzymes are correspondingly very rare in nature, and only one such enzyme has been cloned to date: the farnesylgeranyl diphosphate synthase from *Aeropyrum pernix*, ApFGS (50). We cloned the *apFGS* gene from *A. pernix* genomic DNA, but found it inferior to BstFPS<sub>Y81A</sub> for producing C<sub>25</sub>PP in *E. coli* cells. ApFGS actually behaved more like a C<sub>20</sub>PP synthase with peripheral C<sub>25</sub>PP synthase activity in our carotenogenic *E. coli* (**Figure 3.10**).

In their paper describing the first cloning of ApFGS, Tachibana et al. showed that the enzyme produces a mixture of C<sub>10</sub>PP to C<sub>25</sub>PP products, with C<sub>20</sub>PP being the most abundant, when supplied with the C<sub>5</sub>PP starter unit DMAPP and the C<sub>5</sub>PP extender unit IPP *in vitro* (50). (See **Figure 1.4** for structures.) Only when supplied with C<sub>20</sub>PP did ApFGS exhibit specific C<sub>25</sub>PP synthase ability, but neither the rate nor the extent of the reaction was reported. The extensive production of C<sub>40</sub> carotenoids in *E. coli* expressing ApFGS and CrtM<sub>F26A,W38A</sub> (**Figure 3.10**) appears to stem from the ability of the latter enzyme to incorporate C<sub>20</sub>PP into carotenoids faster than it can be readmitted to ApFGS for further prenyl chain elongation to C<sub>25</sub>PP. A similar effect likely occurs with BstFPS<sub>Y81A</sub>. When supplied with C<sub>15</sub>PP and IPP *in vitro*, this enzyme synthesizes C<sub>25</sub>PP as the major product, with much smaller amounts of C<sub>20</sub>PP being detected (**Figure 3.12** and ref. (37)). However, when BstFPS<sub>Y81A</sub> is coexpressed with a CrtM variant in *E. coli*, significant amounts of C<sub>40</sub> and C<sub>45</sub> carotenoids are synthesized (**Figure 3.8**), indicating that C<sub>20</sub>PP is frequently released by BstFPS<sub>Y81A</sub> *in vivo*. Production of C<sub>20</sub>PP by BstFPS<sub>Y81A</sub> is more common in the elongation of the 5-carbon DMAPP (see below), a substrate also present in *E. coli*. Whereas *in vitro*, released C<sub>20</sub>PP is readily readmitted to BstFPS<sub>Y81A</sub> and extended to C<sub>25</sub>PP (37), in the above cells, BstFPS<sub>Y81A</sub> must compete with a CrtM variant for C<sub>20</sub>PP. Therefore, in *E. coli* cells also expressing CrtM<sub>F26L</sub> or CrtM<sub>F26A,W38A</sub>, much of the C<sub>20</sub>PP released by BstFPS<sub>Y81A</sub> is instead used to synthesize C<sub>40</sub> and C<sub>45</sub> carotenoids. An important lesson from these observations is that the performance of an enzyme *in vitro* may not be representative of its performance as part of an *in vivo* biosynthetic pathway.

In the course of other work aimed at increasing the total quantity of carotenoids synthesized by our cultures, we overexpressed *E. coli* isopentenyl diphosphate isomerase (Idi) along with BstFPS<sub>Y81A</sub> and a CrtM variant on plasmids (**Figure 3.11**). The isomerization of IPP to DMAPP is a rate-limiting step for the production of isoprenoids in *E. coli* (59). IPP is the basic isoprene unit synthesized by both the mevalonate and non-mevalonate pathways of isoprenoid biosynthesis in nature (7). However, IPP serves as an extender unit in prenyl chain elongation, and its isomer, DMAPP, which serves as the starter unit, is only synthesized by Idi-catalyzed isomerization of IPP (7). Overexpression of Idi increases carbon flux to DMAPP, which in turn increases flux through downstream isoprenoid biosynthetic pathways (59).

When we transformed *E. coli* XL1-Blue cells with the plasmids pUC18m-*bstFPS*<sub>Y81A</sub>-*idi* and pAC-*crtM*<sub>F26A,W38A</sub>, the resulting liquid cultures did indeed synthesize about an order of magnitude more total carotenoids compared with XL1-Blue(pUC18m-*bstFPS*<sub>Y81A</sub> + pAC-*crtM*<sub>F26A,W38A</sub>) cultures (**Figure 3.11** caption). However, the distribution of carotenoid backbones was also dramatically shifted toward the production of C<sub>40</sub> carotenoids (**Figure 3.11**). This result can be rationalized by the “statistical” nature of BstFPS<sub>Y81A</sub> and the increased level of DMAPP in cells overexpressing Idi. Five-carbon DMAPP, the smallest isoprenyl diphosphate starter unit, is in addition to C<sub>15</sub>PP and C<sub>20</sub>PP, an acceptable substrate for BstFPS<sub>Y81A</sub> (37). With the isoprenyl diphosphate pool of cells overexpressing Idi enriched in DMAPP, BstFPS<sub>Y81A</sub> will admit this substrate more often. As a “statistical” iterative biocatalyst, BstFPS<sub>Y81A</sub> tends to discharge shorter products on average when supplied with shorter substrates, and indeed, the enzyme frequently releases C<sub>20</sub>PP as it catalyzes prenyl chain elongation starting

from DMAPP (37). It follows that an increased level of DMAPP in the cells will result in increased production of C<sub>20</sub>PP by BstFPS<sub>Y81A</sub>. Since the CrtM variants can condense a variety of prenyl diphosphates into different carotenoids, the larger proportion of C<sub>20</sub>PP in their substrate pool results in the observed shift toward the production of C<sub>40</sub> carotenoids. This example illuminates the importance of the composition of the first enzyme's substrate pool in determining the mixture of end-products of biosynthetic pathways composed of a succession of mutant enzymes with low substrate specificity.

As stated previously, C<sub>50</sub> carotenoids were only desaturated to a relatively small extent *in vivo* by CrtI, and unmetabolized C<sub>50</sub> carotenoid backbones comprised approximately 50 mol% of the carotenoid pool in cultures of XL1-Blue(pUCmodII-*crtM*<sub>F26A,W38A</sub>-*crtI*-*bstFPS*<sub>Y81A</sub>). If we could evolve a desaturase to more efficiently convert C<sub>50</sub> backbones, it might be possible to use colorimetric screening of bacterial colonies in order to further evolve either BstFPS<sub>Y81A</sub> for more specific production of C<sub>25</sub>PP, or to evolve a CrtM variant for more specific synthesis of either C<sub>45</sub> or C<sub>50</sub> carotenoid backbones. Such a screen would require that a given desaturase variant could proficiently desaturate both C<sub>45</sub> and C<sub>50</sub> backbones, and also that the major desaturation product of each pathway be a different color. However, before we could attempt to evolve CrtI or another desaturase for improved performance on a C<sub>50</sub> substrate, we encountered an unexpected roadblock. The first indication of this issue occurred when we noticed that *E. coli* colonies expressing BstFPS<sub>Y81A</sub>, a CrtM variant, and CrtI from one or two plasmids reproducibly displayed a dramatically deeper red color than cell pellets from liquid cultures harboring the same plasmid(s). HPLC analysis revealed that the distribution of carotenoids in our recombinant *E. coli* colonies was shifted toward C<sub>40</sub>

products, with C<sub>50</sub> and C<sub>45</sub> carotenoids each representing less than 10% of total carotenoids (**Figure 3.11**). The similarity of this shift to that brought on by Idi overexpression in liquid cultures leads us to hypothesize that our *E. coli* cells grown in colonies on agar plates contain a higher proportion of DMAPP than cells harboring the same plasmids grown in liquid culture. As we have seen with Idi, such a difference in the relative proportions of C<sub>5</sub>-C<sub>25</sub> prenyl diphosphates between the two physiological states would be sufficient to explain the different carotenoid distributions. However, we can only speculate on the origins of this putative difference in the isoprenyl diphosphate pools of cells cultivated in liquid medium versus those grown on agar plates.

One of our early goals was to generate biosynthetic pathways to C<sub>60</sub> carotenoids. When we formulated that objective, the C<sub>45</sub> and C<sub>50</sub> pathways had not yet been generated, and it was not known for certain which aspects of the C<sub>60</sub> project would be the most problematic. Now, in retrospect, we have substantially more understanding of the experimental bottlenecks to expect. The first step of the pathway, generation of a C<sub>30</sub>PP precursor, has already been discovered by nature. Unlike C<sub>25</sub>PP, C<sub>30</sub>PP is found in bacteria, archaea, and eukaryotes, serving as a precursor to the side chain of quinones (26, 60). Isoprenyl diphosphate synthases that synthesize C<sub>30</sub>PP are therefore rather widespread in nature. The results of our work as well as that of Shimizu et al. with the C<sub>30</sub>PP synthase HexPS from *M. luteus* demonstrate that it is quite efficient and specific at converting C<sub>15</sub>PP to C<sub>30</sub>PP (**Figure 3.12** and ref. (47)).

Despite the ability of HexPS to supply C<sub>30</sub>PP in *E. coli*, enzymes capable of catalyzing C<sub>60</sub> carotenoid backbone synthesis and desaturation remain undiscovered. We found that neither the C<sub>40</sub> synthase CrtB nor CrtM mutants capable of C<sub>50</sub> carotenoid

backbone synthesis could convert C<sub>30</sub>PP into a C<sub>60</sub> backbone. Furthermore, screening for a carotenoid synthase variant capable of producing C<sub>60</sub> backbones will likely not be a simple procedure. Our preferred screening method for evolving carotenoid biosynthetic enzymes, colorimetric screening of colonies, is probably not possible at present in a C<sub>60</sub> pathway, since it cannot be assumed that any known carotenoid desaturase will impart pigmentation on a C<sub>60</sub> backbone. We believe it is unlikely that any wild-type carotenoid desaturase would detectably desaturate a C<sub>60</sub> substrate, since even processing of C<sub>50</sub> backbones poses a great challenge to the broad-specificity desaturase CrtI. On the other hand, if a C<sub>60</sub> carotenoid synthase were to be discovered first, screening for a desaturase variant capable of accepting C<sub>60</sub> backbones should be relatively straightforward. Since C<sub>30</sub>PP is the only substrate available for carotenoid biosynthesis in *E. coli* expressing HexPS, C<sub>60</sub> carotenoid backbones should be the only carotenoids possible in cells expressing HexPS and a C<sub>60</sub> synthase. Therefore, screening *E. coli* colonies additionally transformed with a library of variant desaturases for the emergence of color should be a reliable method to search for desaturase variants capable of converting C<sub>60</sub> backbones into pigmented C<sub>60</sub> products.

The production of hydroxylated carotenoid backbones we have reported in this work is an example of another type of hurdle to pathway specificity that can be encountered by metabolic pathway engineers. Although assembling and coexpressing a series of foreign biosynthetic genes in a heterologous host may look simple on paper, it is not possible to predict all the unwanted side reactions that might occur in the complex environment of a living cell. As we have shown, even *E. coli*, the most studied of all organisms, will carry out unexpected chemical modification of the products of foreign

biosynthetic genes it is forced to express. This is probably especially common when such products are harmful to the cell in some way and elicit poorly understood “emergency” responses. Therefore, given the current state of the art in the heterologous production of small molecules in microorganisms, the old adage, “expect the unexpected” is definitely sage advice.

## CONCLUSIONS

The complexity and variety of small molecules in nature is a testament to the power of evolution to innovate and diversify. Our experiments on carotenoid biosynthetic enzymes and pathways represent an attempt to simultaneously harness and study these remarkable features of evolution. By capturing entire new pathways in the very earliest stages of their emergence, we have learned that new enzyme specificities are discovered rather easily upon mutation, and that new chemical diversity generated early in a pathway can be multiplied by downstream enzymes via many different chemical mechanisms. It is likely that our nascent pathways resemble their counterparts in nature in their rapid gain of access to a variety of new products upon very limited genetic change. However, the evolutionary “pruning” process by which the unwanted majority of a nascent pathway’s products are discarded in favor of a desired few remains unreproduced in the laboratory and, consequently, less well understood. Therefore, the generation of new pathways in the laboratory by directed evolution of biosynthetic enzymes, especially those located early in a pathway, remains primarily a tool for molecular discovery. It is hoped that future directed evolution experiments will shed light on how biosynthetic pathways shift their focus toward the synthesis of advantageous new products. If such research proves

fruitful, the exciting prospect of a commercial-scale whole-cell process for the specific production of a useful new molecule originally discovered in the laboratory by directed evolution may become a reality.

## MATERIALS AND METHODS

### Genes and plasmids

Plasmid maps and sequences can be found in Appendix A. Genes are listed in transcriptional order in the names of all the plasmids in this report. Plasmids based on the high-copy pUCmodII vector (46, 54) are designated by names beginning with “pUCmodII.” The carotenoid biosynthetic genes on these plasmids are expressed as an operon under the control of a single *lac* promoter with no *lac* operator. In plasmids pUCmodII-*crtM*<sub>F26L</sub>-*bstFPS*<sub>Y81A</sub> and pUCmodII-*crtM*<sub>F26A,W38A</sub>-*bstFPS*<sub>Y81A</sub>, a variant of the C<sub>30</sub> carotenoid synthase gene *crtM* from *Staphylococcus aureus* (*crtM*<sub>F26L</sub> or *crtM*<sub>F26A,W38A</sub>, respectively (54-56)) is flanked by *Xba*I and *Xho*I restriction sites. *bstFPS*<sub>Y81A</sub>, which encodes the Y81A mutant of the farnesyl diphosphate synthase from *Bacillus stearothermophilus* (37, 54), is flanked by *Eco*RI and *Nco*I restriction sites and directly follows the *crtM* variant. Plasmids pUCmodII-*crtM*<sub>F26L</sub>-*crtI*-*bstFPS*<sub>Y81A</sub> and pUCmodII-*crtM*<sub>F26A,W38A</sub>-*crtI*-*bstFPS*<sub>Y81A</sub> additionally contain the gene encoding the carotenoid desaturase *CrtI* from *Erwinia uredovora* (current approved name: *Pantoea ananatis*), which is inserted between the *crtM* and *bstFPS* variants and is flanked by *Xho*I and *Eco*RI restriction sites. Plasmid pUCmodII-*crtI*, used to express *E. uredovora* *CrtI* alone for *in vitro* desaturation experiments, contains *crtI* flanked by *Eco*RI and *Nco*I restriction sites.

The genes on plasmids based on the high-copy vector pUC18m (56) are expressed as an operon under the control of a *lac* promoter and operator. Plasmid pUC18m-*bstFPS*<sub>Y81A</sub> contains the *bstFPS*<sub>Y81A</sub> gene flanked by *Xba*I and *Xho*I restriction sites. Plasmid pUC18m-*bstFPS*<sub>Y81A</sub>-*idi* additionally contains the *idi* gene encoding *E. coli* isopentenyl diphosphate isomerase, which is inserted between *Xho*I and *Apa*I restriction sites. Plasmid pUC18m-*crtM*<sub>F26A,W38A</sub> contains *crtM*<sub>F26A,W38A</sub> flanked by *Xba*I and *Xho*I sites. We cloned *apFGS*, the FGPP (C<sub>25</sub>PP) synthase gene from *Aeropyrum pernix* (50) from *A. pernix* genomic DNA (ATCC no. 700893D) by PCR. pUC18m-*apFGS* contains the *apFGS* gene flanked by *Nde*I and *Eco*RI sites. Plasmid pUC18m-*apFGS*-*crtM*<sub>F26A,W38A</sub> additionally contains *crtM*<sub>F26A,W38A</sub> flanked by *Xba*I and *Xho*I sites. Plasmid pUC18m-*hexPS* contains the operon from *Micrococcus luteus* strain B-P 26 encoding the two polypeptide components of hexaprenyl diphosphate (C<sub>30</sub>PP) synthase (47). This operon, referred to as “*hexPS*,” is flanked by *Eco*RI and *Xba*I restriction sites. pUC18m-*hexPS*-*crtM*-*crtN* additionally includes wild-type *crtM* flanked by *Xba*I and *Xho*I sites and *crtN*, the *S. aureus* C<sub>30</sub> carotenoid desaturase gene, between *Xho*I and *Apa*I sites. In plasmid pUC18m-*crtM*-*crtN*, *crtM* and *crtN* are flanked by the same sites as in pUC18m-*hexPS*-*crtM*-*crtN*. Plasmid pUC18m-*hexPS*-*crtB*-*crtI* has the same construction as pUC18m-*hexPS*-*crtM*-*crtN* but contains *crtB*, the C<sub>40</sub> carotenoid synthase gene from *E. uredovora*, in place of *crtM* and *crtI* from the same bacterium in place of *crtN*. The plasmids pUC18m-*hexPS*-*crtM*<sub>F26L</sub> and pUC18m-*hexPS*-*crtM*<sub>F26A,W38A</sub> have the same construction as pUC18m-*hexPS*-*crtM*-*crtN* but lack *crtN*. pUC18m-*hexPS*-*crtB* is the same as pUC18m-*hexPS*-*crtB*-*crtI* but lacks *crtI*, while plasmid pUC18m-*crtE*-*crtB*-*crtI*

has the same construction as pUC18m-*hexPS-crtB-crtI* but has *crtE*, the gene encoding the GGPP (C<sub>20</sub>PP) synthase from *E. uredovora*, in place of *hexPS*.

Plasmids based on the medium-copy vector pACmod (pACYC184 with the *XbaI* site removed) (46) were constructed by insertion of a fragment containing the entire operon from a pUC18m-based plasmid (including the *lac* promoter and operator) into pACmod. In plasmid pAC-*crtM*<sub>F26A,W38A</sub>, *crtM*<sub>F26A,W38A</sub> is inserted between *XbaI* and *XhoI* restriction sites. In pAC-*crtM*<sub>F26A,W38A</sub>-*crtI*, *crtI* from *E. uredovora* is also present and is flanked by *XhoI* and *ApaI* sites. Plasmid pAC-*crtE* contains *crtE* flanked by *EcoRI* and *XbaI* sites.

In all plasmids listed above, an optimized Shine-Dalgarno ribosomal binding sequence (AGGAGG) followed by eight spacer nucleotides is situated directly upstream of each gene's start codon. Even for the plasmids with *lac* operator sequences, leaky transcription was sufficient to effect the expression of carotenogenic genes. Therefore, all experiments described in this report were performed without IPTG (isopropyl-β-D-thiogalactopyranoside) induction.

### **Bacterial cultures and carotenoid extraction**

*E. coli* XL1-Blue cells (Stratagene, La Jolla, CA) were transformed with plasmid DNA and plated on Luria-Bertani (LB)-agar plates supplemented with 50 mg/l of each appropriate antibiotic (carbenicillin for pUC-based plasmids, chloramphenicol for pAC-based plasmids). Colonies were usually visible after 12 h at 37 °C, at which point 2-ml precultures of LB+antibiotics (50 mg/l each) were inoculated with single colonies and shaken at 37 °C and 250 rpm for 12-18 h. One milliliter of preculture was inoculated into 1 liter of Terrific broth (TB)+antibiotics (50 mg/l each) in a 2.8-liter Erlenmeyer flask.

One-liter cultures were shaken at 28 °C and 250 rpm for 48 h. Optical densities at 600 nm of 1-liter cultures ( $OD_{600nm}$ ) were measured after 10-fold dilution into fresh TB medium. Dry cell masses were determined from  $OD_{600nm}$  values using a calibration curve generated for XL1-Blue cultures.

Cells were pelleted by centrifugation at  $2500 \times g$  for 15 min. For accurate quantification of total carotenoid titers, a known amount of  $\beta,\beta$ -carotene (Fluka/Sigma, St. Louis, MO) was added to pellets as an internal standard before extraction. Cell lysis and initial carotenoid extraction was achieved by addition of 100 ml of acetone supplemented with 30 mg/l of 3,5-di-*tert*-butyl-4-hydroxytoluene (BHT; Sigma) followed by vigorous shaking. After this point, to avoid difficulties with mass spectrometry (MS), contact with plasticware was avoided and only glassware was used. After filtration and concentration to ~5 ml under a stream of  $N_2$ , lipids including carotenoids were partitioned twice into 8 ml of hexanes and then concentrated to ~4 ml under a stream of  $N_2$ . This extract was then washed 5 times with 2 ml of deionized water, dewatered with anhydrous  $MgSO_4$ , filtered, and then evaporated to dryness under a stream of  $N_2$ . After resuspension in 2 ml of acetone + BHT (30 mg/l), a significant amount of fatty material usually precipitated on the sides of the vial. The mixture was sonicated at 40 °C for 10-20 min. to dissolve carotenoids trapped by the precipitate and was then filtered and evaporated to dryness under a stream of  $N_2$ . Dried extracts were stored under argon gas at -20 °C. Extracts were dissolved into 0.1-1 ml of acetonitrile prior to separation and analysis.

For analysis of carotenoids synthesized by *E. coli* colonies, LB-agar plates were removed from 37 °C after colonies had formed (usually 12 h). The plates were incubated

at 25 °C for 48 h to promote carotenoid biosynthesis. Colonies were lifted onto white nitrocellulose membranes (Pall, Port Washington, NY) for imaging on a flatbed scanner. For extraction of carotenoids from colonies, TB medium was used to suspend the colonies, after which the mixture was centrifuged at  $2500 \times g$  for 15 min. After decanting the liquid, dry cell masses were determined from measured wet cell masses using a calibration curve generated for XL1-Blue cells. The same steps listed above for carotenoid extraction from liquid culture pellets were followed but all volumes were scaled by a factor of 0.2 due to the smaller cell pellets obtained from scraping colonies compared with pellets from liquid cultures. We generally found that ~0.5 g of wet cells was sufficient to obtain enough extract for HPLC analysis.

### **Separation and analysis of carotenoids**

The above extracts dissolved in acetonitrile were injected into an Xterra MS C<sub>18</sub> column (3.0 × 150 mm, 3.5- $\mu$ m particle size; Waters, Milford, MA) outfitted with a guard cartridge (3.0 × 20 mm, identical particles) using an Alliance 2690 HPLC system (Waters) equipped with a photodiode array detector (PDA) set to 1.2-nm resolution. For isocratic elution, the mobile phase was acetonitrile:isopropanol 93:7 (by volume) and the flowrate was 0.4 ml/min. For more rapid elution of highly nonpolar C<sub>45</sub> and C<sub>50</sub> carotenoids, a gradient method with the same flowrate was employed: 0-35 min, acetonitrile:isopropanol 93:7; 35-37 min, linear gradient to acetonitrile:isopropanol 50:50; 37-50 min, acetonitrile:isopropanol 50:50. Carotenoids injected to HPLC were quantified by comparing their chromatogram peak areas (determined at the wavelength of maximum absorption for each carotenoid in the sample) to a calibration curve generated using known amounts of  $\beta,\beta$ -carotene and then multiplying by the ratio of molar

extinction coefficients ( $\epsilon_{\beta, \beta\text{-carotene}}/\epsilon_{\text{sample carotenoid}}$ ) (9). The calibration curve and internal standard peak areas enabled the calculation of scaling factors, which permitted the computation of total carotenoid titers from the HPLC data.

Fractions of the HPLC eluent containing separated carotenoids were collected and evaporated to dryness under  $N_2$ . Mass spectra of carotenoids were obtained using either an 1100 Series HPLC-PDA-MS system (Hewlett Packard/Agilent, Palo Alto, CA) equipped with an atmospheric pressure chemical ionization (APCI) interface or a Finnigan LCQ mass spectrometer equipped with an electrospray ionization (ESI) source (Thermo Electron, San Jose, CA). Previously separated carotenoids were resuspended in either hexanes (for APCI-MS) or methanol:dichloromethane 85:15 (by volume) (for ESI-MS) and flow-injected into the mobile phase, which was the same as the solvent used to dissolve the sample.

Carotenoids were identified and the putative structures of novel carotenoids were assigned based on their HPLC retention times, UV-visible spectra, and mass spectra.

### **Acetylation of hydroxylated carotenoid backbones**

To confirm the presence of a hydroxy group on carotenoid backbones, the acetylation protocol suggested by Eugster (19) was followed with slight modification. Briefly, 5-10 nmol of a hydroxylated carotenoid backbone was dissolved in 0.5 ml of pyridine (dried over BaO powder). Fifty microliters of acetic anhydride was then added, and the reactions were carried out at room temperature for 1 h. The reactions were terminated by addition of 4 ml of deionized water, and carotenoids were extracted by partitioning twice with 1 ml of hexanes. After evaporation of the solvent under a stream of  $N_2$ , the product mixture was analyzed and separated by HPLC as described above. The

separated product and unreacted fractions were dried under N<sub>2</sub>, resuspended in hexanes, and analyzed by APCI-MS as described above.

### ***In vitro* desaturation of carotenoid backbones**

Cell lysate of *E. coli* cultures expressing CrtI was prepared for *in vitro* desaturation reactions as follows. 150-ml cultures of XL1-Blue(pUCmodII-*crtI*) were shaken in TB medium supplemented with carbenicillin (50 mg/l) at 28 °C and 113 rpm in upright 175 cm<sup>2</sup> tissue culture flasks (BD Falcon, Bedford, MA) until they reached an OD<sub>600nm</sub> of 5-6 (~48 h). Cells were centrifuged at 2500 × *g* for 15 min., and each pellet from a 150-ml culture was resuspended in 20 ml of Tris-HCl buffer (50 mM, pH 8) containing 1 mM phenylmethylsulfonylfluoride (PMSF). Cells were lysed by French press, and the lysate was stored at -20 °C in 1-ml aliquots until use.

Carotenoid backbone substrates for *in vitro* desaturation reactions were separated and purified as described above from cultures of XL1-Blue(pUCmodII-*crtM*<sub>F26L</sub>-*bstFPS*<sub>Y81A</sub>), XL1-Blue(pUCmodII-*crtM*<sub>F26A,W38A</sub>-*bstFPS*<sub>Y81A</sub>), or XL1-Blue(pUC18m-*crtE-crtB*) (synthesizing authentic phytoene only (56)). After resuspension in a known amount of hexanes, carotenoid backbones were quantified by their absorbance at 286 nm using a Cary 100 Bio UV-visible spectrophotometer (Varian, Palo Alto, CA). For each *in vitro* desaturation reaction, 10 nmol of a carotenoid backbone was resuspended in 10 μl of acetone and added to a thawed 1-ml aliquot of XL1-Blue(pUCmodII-*crtI*) lysate supplemented with additional flavin adenine dinucleotide (FAD, 1mM) and MgCl<sub>2</sub> (4 mM). Reaction mixtures were then incubated at 30 °C with gentle end-over-end rotation for 12-18 h.

To extract carotenoids from *in vitro* reactions for HPLC analysis, the reaction mixtures were centrifuged at  $14,000 \times g$  for 5 min. and the pellets were separated from the supernatants. Pellets were extracted with 1 ml of acetone + BHT (30 mg/l), thoroughly vortexed, and then filtered. Carotenoids were extracted from the aqueous supernatants by partitioning twice with 1 ml of hexanes. The hexane and acetone extracts of each reaction mixture were pooled and evaporated to dryness under a stream of  $N_2$ . Carotenoids were then resuspended in 150  $\mu$ l of acetonitrile and analyzed by HPLC as described above.

### **Iodine-catalyzed photoisomerization**

To enrich mixtures of *E*- and *Z*-carotenoids in all-*E* (*trans*) isomers or verify the all-*E* configuration of specific carotenoids, individual carotenoids or culture extracts were subjected to iodine-catalyzed photoisomerization following the protocol suggested by Schiedt and Liaaen-Jensen (44). After photoisomerization, samples were analyzed by HPLC and changes in *E/Z* isomeric configuration were identified by the bathochromic (or hypsochromic) shifts in their absorption spectra and the intensity change of *cis*-peaks (9) compared with control samples not subjected to photoisomerization.

### **Thin-layer chromatography and autoradiography analysis of isoprenyl diphosphate synthase reactions**

*In vitro* investigations of isoprenyl diphosphate synthase reactions were performed by Adam Hartwick as follows. *E. coli* XL1-Blue cells transformed with pUC18m-*crtE*, pUC18m-*bstFPS*<sub>Y81A</sub>, or pUC18m-*hexPS* were cultured for 24 h in 100 ml of TB medium supplemented with carbenicillin (50 mg/l) at 37 °C in 500-ml Erlenmeyer

flasks shaken at 250 rpm for 24 h. Each culture was divided into 4 equal aliquots, which were centrifuged at 4 °C for 10 min. at  $3000 \times g$ . The cell pellets were stored at -80 °C. Pellets were thawed on ice and then resuspended in 5 ml of Tris-HCl buffer (25 mM, pH 8.5) supplemented with 1 mM EDTA and 10 mM 2-mercaptoethanol. The resuspended cells were lysed by microtip sonication and then centrifuged at  $4500 \times g$  for 20 min. The supernatants were stored in 250- $\mu$ l aliquots at -80 °C until use.

Enzyme reactions were carried out by mixing the following: 100  $\mu$ l of reaction buffer (50 mM HEPES buffer, pH 8.2 supplemented with 40 mM  $MgCl_2$ , 40 mM  $MnCl_2$ , and 200 mM 2-mercaptoethanol), 100  $\mu$ l of FPP ( $C_{15}PP$ ) buffer (100  $\mu$ M FPP in 25 mM HEPES buffer, pH 8.2), 100  $\mu$ l of  $^{14}C$ -IPP buffer (12  $\mu$ M  $^{14}C$ -labeled IPP in 25 mM HEPES buffer, pH 8.2), and 100  $\mu$ l of one of the above lysates. The reaction mixtures were shaken at 37 °C and 1000 rpm for 4 h.

Radiolabeled isoprenyl diphosphate products were extracted from the reactions by addition of 200  $\mu$ l of 1-butanol followed by vortexing and centrifugation at  $14000 \times g$  for 30 sec. The butanol epiphase was withdrawn and used directly in the subsequent dephosphorylation reaction by potato acid phosphatase (Sigma). The butanol extracts were combined with 400  $\mu$ l of methanol, 100  $\mu$ l of acetate buffer (1 M, pH 5.6), 100  $\mu$ l of 1% (w/v) Triton X-100, and 200  $\mu$ l of acid phosphatase buffer (44 units enzyme/ml in acetate buffer). The dephosphorylation reactions were then shaken at 37 °C and 1000 rpm for 24 h.

Following dephosphorylation,  $^{14}C$ -labeled isoprenyl alcohols were extracted with 0.1 ml of n-pentane. After vortexing and centrifugation, the organic layer was removed by pipette. A portion of each pentane extract was spotted onto a  $C_{18}$  reverse-phase TLC

plate, which was developed with a mobile phase of acetone:water 9:1 (by volume). TLC plates were then exposed to a phosphor plate for ~24 h. Autoradiogram images were obtained by scanning the phosphor plates with a Typhoon Imager (Amersham).

**Table 3.1.** Properties of novel desaturated carotenoids synthesized by XL1-Blue(pUCmodII-*crtM*<sub>F26A,W38A</sub>-*crtI*-*bstFPS*<sub>Y81A</sub>)

Backbone	Conjugated double bonds	Retention time <sup>a</sup> (min)	Molecular ion ( <i>m/z</i> ) <sup>b</sup>	Mol% <sup>c</sup>	UV-visible spectrum (Fig. 3.6) and putative structure (Figs. 3.2-3.4)
C <sub>40</sub>	7	19.2	540.2	5	<b>1</b>
C <sub>45</sub>	7	30.0	608.4	0.5	<b>3</b>
C <sub>45</sub>	9	28.5	606.2	1	<b>4</b>
C <sub>45</sub>	13	15.6, 16.4	602.0	4	<b>5</b>
C <sub>45</sub>	15	13.9	600.2	2	<b>6</b>
C <sub>50</sub>	7	42.0	676.2	2	<b>10</b>
C <sub>50</sub>	9	39.6, 40.4	674.2	5	<b>11a</b>
C <sub>50</sub>	9	38.0	674.2	0.5	<b>11b</b>
C <sub>50</sub>	11	35.9	672.3	3	<b>12a</b>
C <sub>50</sub>	11	34.8	672.3	2	<b>12b/c</b>
C <sub>50</sub>	15	20.3, 21.4	668.1	5	<b>13</b>

a. Using the column and gradient method described in Materials and Methods. Multiple times refer to *E/Z* isomers of the same carotenoid.

b. Determined by electrospray mass spectrometry. Carotenoids underwent direct electrochemical oxidation to give the radical molecular cation [M·]<sup>+</sup>.

c. Approximate, of all carotenoids detected in the culture extract by HPLC.

Unmetabolized 16,16'-diisopentenylphytoene (C<sub>50</sub> backbone) represented ~50 mol% of this population.

**Table 3.2.** Names of numbered carotenoid structures depicted in Figures 3.2-3.4

Structure number	Trivial name <sup>a</sup>	IUPAC-IUB semi-systematic name
<b>1</b>	16-isopentenyl-7,8,11,12-tetrahydro-4'-apocyclopene	16-(3-methylbut-2-enyl)-7,8,11,12-tetrahydro-4'-apo- $\psi,\psi$ -carotene
<b>2a</b>	C <sub>45</sub> -phytofluene (9-13')	16-(3-methylbut-2-enyl)-7,8,7',8',11',12'-hexahydro- $\psi,\psi$ -carotene
<b>2b</b>	C <sub>45</sub> -phytofluene (13-9')	16-(3-methylbut-2-enyl)-7,8,11,12,7',8'-hexahydro- $\psi,\psi$ -carotene
<b>3</b>	C <sub>45</sub> - $\zeta$ -carotene	16-(3-methylbut-2-enyl)-7,8,7',8'-tetrahydro- $\psi,\psi$ -carotene
<b>4a</b>	C <sub>45</sub> -neurosporene (5-9')	16-(3-methylbut-2-enyl)-7',8'-dihydro- $\psi,\psi$ -carotene
<b>4b</b>	C <sub>45</sub> -neurosporene (9-5')	16-(3-methylbut-2-enyl)-7,8-dihydro- $\psi,\psi$ -carotene
<b>5a</b>	C <sub>45</sub> -didehydrolycopene (1-5')	16-(3-methylbut-2-enyl)-3,4-didehydro- $\psi,\psi$ -carotene
<b>5b</b>	C <sub>45</sub> -didehydrolycopene (5-1')	16-(3-methylbut-2-enyl)-3',4'-didehydro- $\psi,\psi$ -carotene
<b>6</b>	C <sub>45</sub> -tetrahydrolycopene (1-1')	16-(3-methylbut-2-enyl)-3,4,3',4'-tetrahydro- $\psi,\psi$ -carotene
<b>10</b>	C <sub>50</sub> - $\zeta$ -carotene	16,16'-di-(3-methylbut-2-enyl)-7,8,7',8'-tetrahydro- $\psi,\psi$ -carotene
<b>11a</b>	C <sub>50</sub> -neurosporene (5-9')	16,16'-di-(3-methylbut-2-enyl)-7,8-dihydro- $\psi,\psi$ -carotene
<b>11b</b>	C <sub>50</sub> -neurosporene (1-13')	16,16'-di-(3-methylbut-2-enyl)-3,4-didehydro-7',8',11',12'-tetrahydro- $\psi,\psi$ -carotene
<b>12a</b>	C <sub>50</sub> -lycopene (5-5')	16,16'-di-(3-methylbut-2-enyl)- $\psi,\psi$ -carotene
<b>12b</b>	C <sub>50</sub> -lycopene (9-1')	16,16'-di-(3-methylbut-2-enyl)-3,4-didehydro-7',8'-dihydro- $\psi,\psi$ -carotene
<b>12c</b>	C <sub>50</sub> -lycopene (13-3'')	16-(3-methylbut-2-enylidene),16'-(3-methylbut-2-enyl)-3,4-didehydro-7',8',11',12'-dihydro- $\psi,\psi$ -carotene
<b>13</b>	C <sub>50</sub> -tetrahydrolycopene	16,16'-di-(3-methylbut-2-enyl)-3,4,3',4'-tetrahydro- $\psi,\psi$ -carotene

a. Numbers in brackets refer to the carbon atoms that mark the ends of the conjugated double-bond system. The double prime in the trivial name for carotenoid **12c** refers to the numbering of the 3-methylbut-2-enylidene group on the right side of the molecule as shown in Figure 3.3.

**Table 3.3.** Results of *in vitro* desaturation experiments with XL1-Blue(pUCmodII-*crtI*) lysate on various carotenoid backbones<sup>a</sup>

Backbone	Conversion (%)	Desaturation products (mol% of product mixture)			
		1-step	2-step	3-step	4-step
C <sub>30</sub>	1	28	41	9	22
phytoene <sup>b</sup>	19	14	13 <sup>c</sup>	7	66
C <sub>40</sub> -OH <sup>d</sup>	30	11	12	19	58
C <sub>45</sub>	5	71 [2] <sup>e</sup>	29 [3]	–	–
C <sub>45</sub> -OH [7]	14	48 [8]	52 [9]	–	–
C <sub>50</sub>	0	–	–	–	–
C <sub>50</sub> -OH [14]	0	–	–	–	–

Numbers in square brackets refer to products shown in Figures 3.2 and 3.5.

- a. Values represent the average of at least two independent experiments rounded to the closest percentage point. Coefficients of variation were less than 0.25.
- b. The native substrate of *CrtI* and positive control. Phytoene was purified from cultures of XL1-Blue(pUC18m-*crtE-crtB*) (56), which produces authentic phytoene only.
- c. Identified by its absorbance spectrum as  $\zeta$ -carotene.
- d. Most likely predominantly OH-phytoene but may have contained some hydroxylated 16-isopentenyl-4'-apophytoene (asymmetric C<sub>40</sub> backbone).
- e. This product was detected only from *in vitro* desaturation of 16-isopentenylphytoene (C<sub>45</sub> backbone) and was not found *in vivo*.

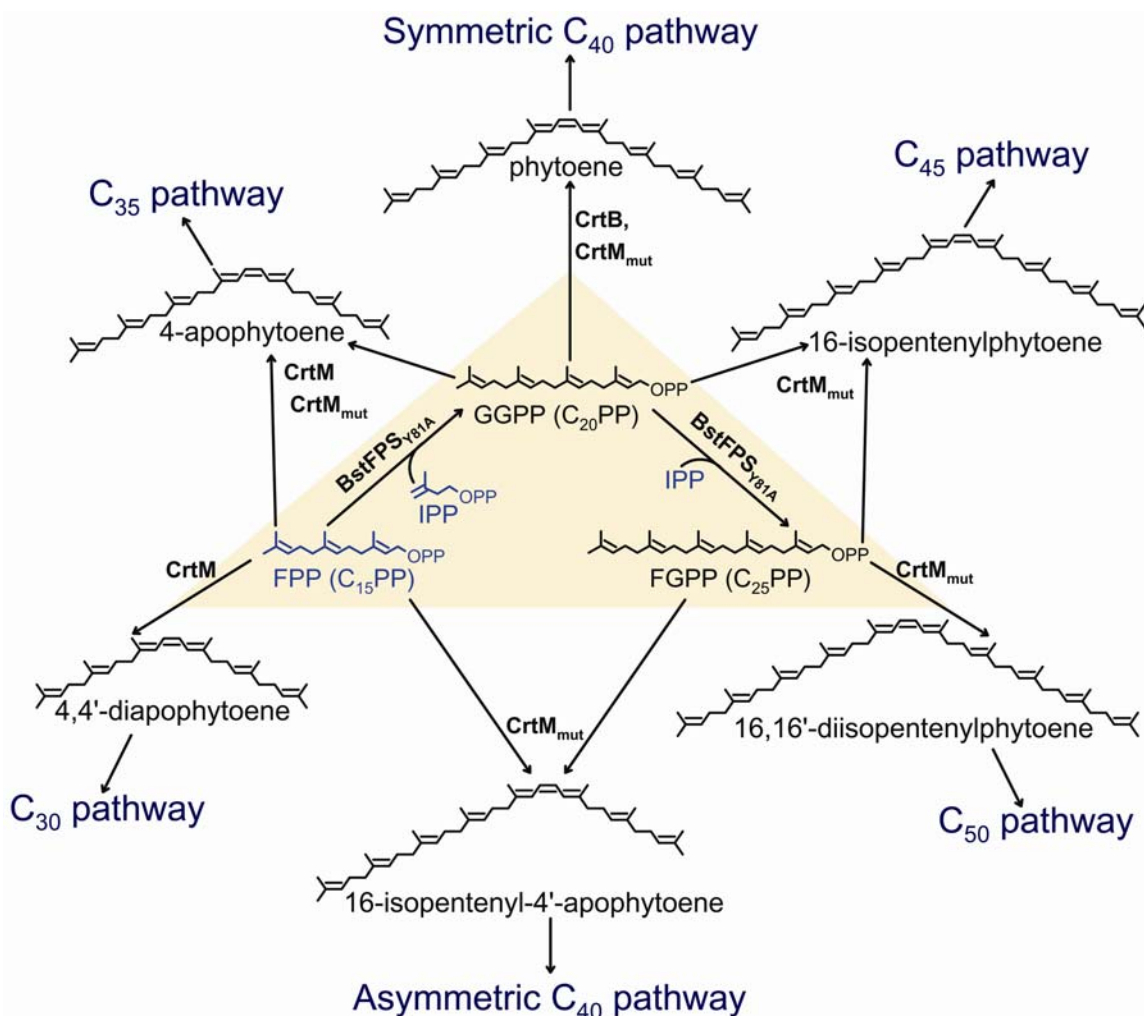


**Figure 3.1. Six carotenoid biosynthetic pathways from three prenyl diphosphate precursors.** Only the C<sub>30</sub> and symmetric C<sub>40</sub> pathways synthesized from C<sub>15</sub>PP and C<sub>20</sub>PP, respectively, have been identified in nature. *E. coli* cells expressing BstFPS<sub>Y81A</sub> synthesize the rare C<sub>25</sub>PP precursor FGPP, which can be incorporated into three unnatural carotenoid backbones—C<sub>45</sub>, C<sub>50</sub> (54), and asymmetric C<sub>40</sub>—upon coexpression of one of a number of CrtM mutants with altered specificity, CrtM<sub>mut</sub>. Wild-type and variants of CrtM can also synthesize C<sub>35</sub> carotenoids by fusion of C<sub>15</sub>PP and C<sub>20</sub>PP as reported previously (53, 56). Prenyl diphosphate precursors endogenous to *E. coli* are depicted in blue. Carotenoid backbones are depicted as the 15Z isomer synthesized by these bacterial carotenoid synthases. CrtB, phytoene synthase; IPP, isopentenyl diphosphate; FPP, farnesyl diphosphate; GGPP, geranylgeranyl diphosphate; FGPP, farnesylgeranyl diphosphate.

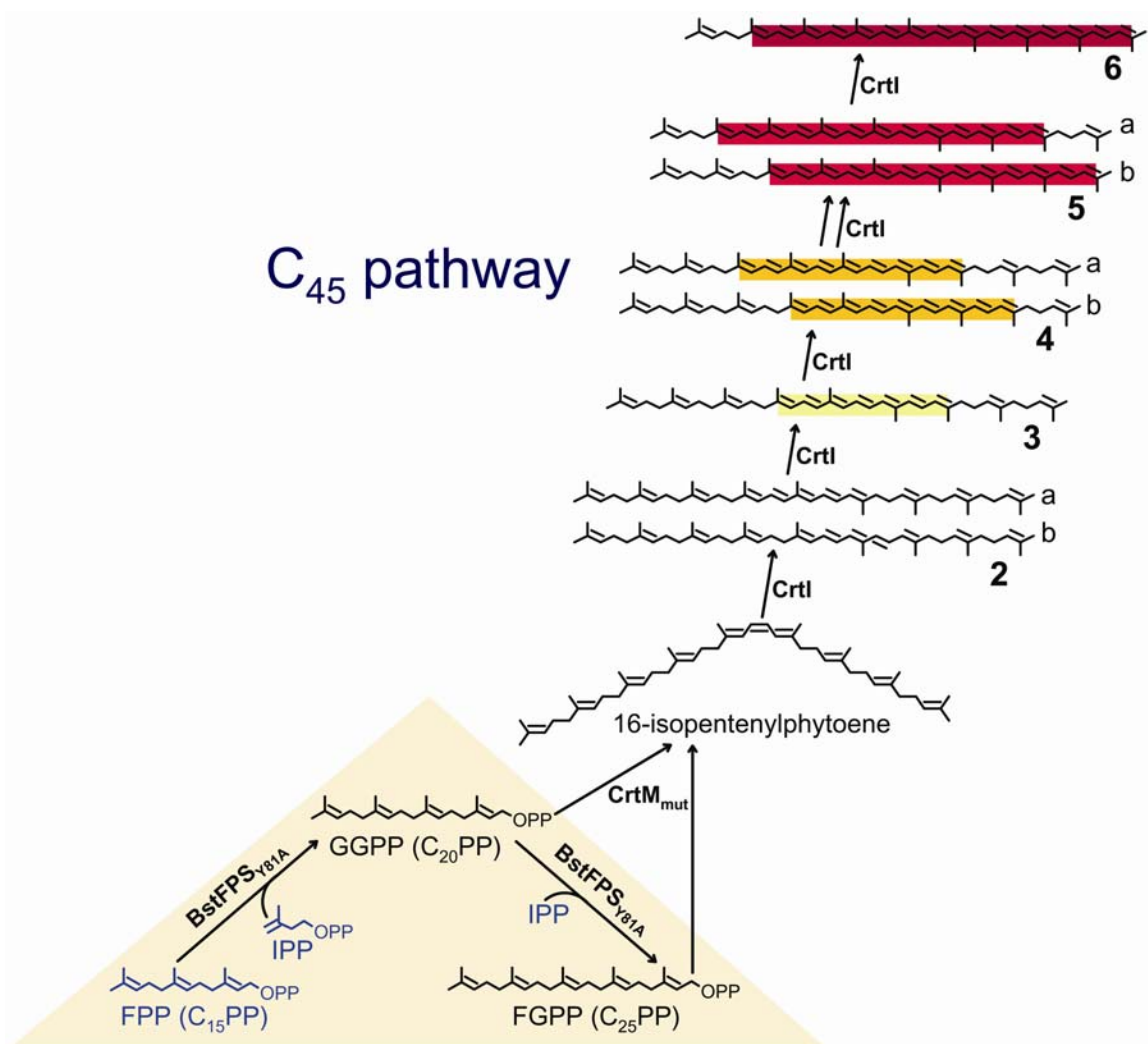


**Figure 3.2. Desaturation in the C<sub>45</sub> pathway.** Simultaneous coexpression of BstFPS<sub>Y81A</sub>, CrtM<sub>F26L</sub> or CrtM<sub>F26A,W38A</sub> (CrtM<sub>mut</sub>), and the carotenoid desaturase CrtI from *E. uredo* resulted in the biosynthesis of desaturated C<sub>45</sub> carotenoids with putative structures 3, 4, 5, and 6, reported for the first time in this work. Carotenoid 2 was only detected from *in vitro* desaturation of 16-isopentenylphytoene. Colored boxes highlighting carotenoid chromophores depict the approximate color of the molecule in white light. Double arrows signify two desaturation steps. Structure numbers (and letters for different desaturation isomers) are used throughout the text and other figures. Names for the numbered structures are listed in Table 3.2. Prenyl diphosphate precursors endogenous to *E. coli* are depicted in blue. IPP, isopentenyl diphosphate; FPP, farnesyl diphosphate; GGPP, geranylgeranyl diphosphate; FGPP, farnesylgeranyl diphosphate.

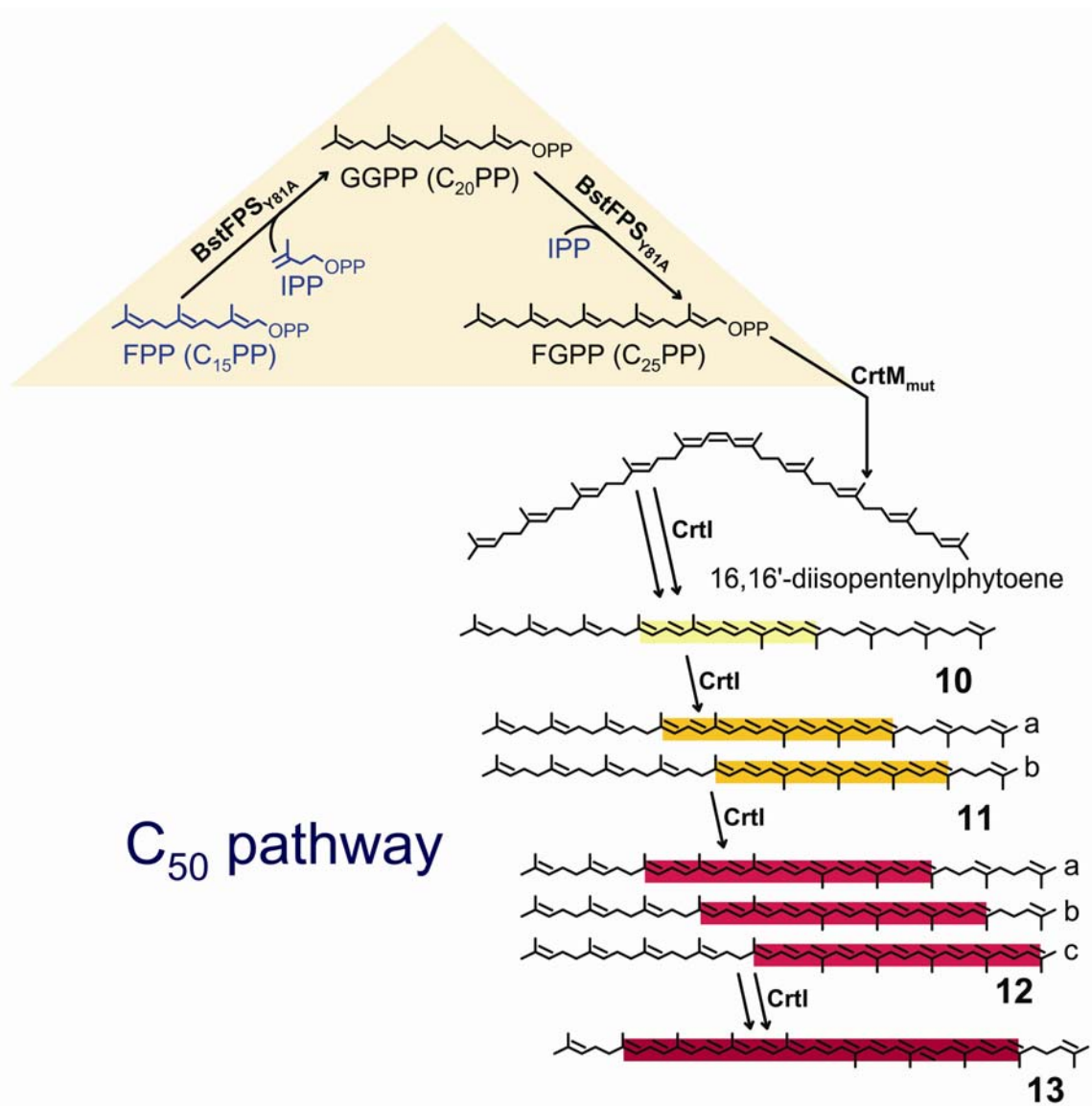


Figure 3.3

**Figure 3.3. Desaturation in the C<sub>50</sub> pathway.** Simultaneous coexpression of BstFPS<sub>Y81A</sub>, CrtM<sub>F26L</sub> or CrtM<sub>F26A,W38A</sub> (CrtM<sub>mut</sub>), and the carotenoid desaturase CrtI from *E. uredoovora* resulted in the biosynthesis of desaturated C<sub>50</sub> carotenoids with putative structures **10**, **11**, **12**, and **13**, reported for the first time in this work. Colored boxes highlighting carotenoid chromophores depict the approximate color of the molecule in white light. Double arrows signify two desaturation steps. Structure numbers (and letters for different desaturation isomers) are used throughout the text and other figures. Names for the numbered structures are listed in Table 3.2. Prenyl diphosphate precursors endogenous to *E. coli* are depicted in blue. IPP, isopentenyl diphosphate; FPP, farnesyl diphosphate; GGPP, geranylgeranyl diphosphate; FGPP, farnesylgeranyl diphosphate.

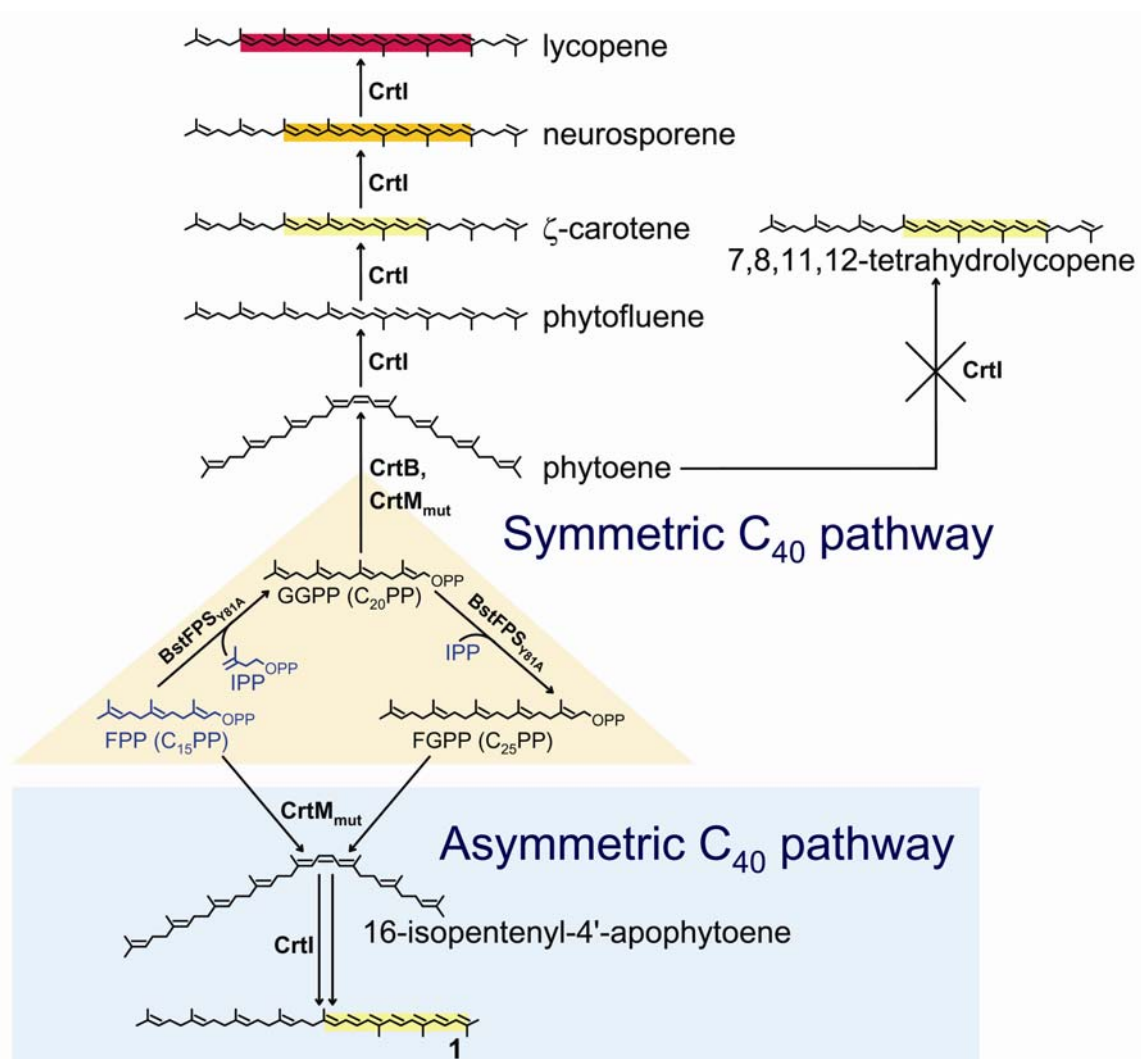


Figure 3.4

**Figure 3.4. An asymmetric C<sub>40</sub> pathway.** Simultaneous coexpression of BstFPS<sub>Y81A</sub>, CrtM<sub>F26L</sub> or CrtM<sub>F26A,W38A</sub> (CrtM<sub>mut</sub>), and the carotenoid desaturase CrtI from *E. uredovora* resulted in the biosynthesis of 2-step carotenoid **1**, putatively the first carotenoid from the novel asymmetric C<sub>40</sub> carotenoid biosynthetic pathway (blue shading) to be isolated. Several lines of evidence support the precise structure of **1** (named in Table 3.2) shown in the figure, including its biosynthesis via 2+0 desaturation of an asymmetric C<sub>40</sub> carotenoid backbone formed by condensation of C<sub>15</sub>PP and C<sub>25</sub>PP (see Discussion). Symmetric C<sub>40</sub> pathway carotenoids phytoene, phytofluene, ζ-carotene, neurosporene, and lycopene are shown for comparison; lycopene was also detected in the same cultures as **1**. The structure of 7,8,11,12-tetrahydrolycopene, with the same 2+0 desaturation pattern as **1**, is also shown for comparison. This carotenoid is not known to be made by *E. uredovora* CrtI (crossed-out arrow). Colored boxes highlighting carotenoid chromophores depict the approximate color of the molecule in white light. Prenyl diphosphate precursors endogenous to *E. coli* are depicted in blue. CrtB, phytoene synthase; IPP, isopentenyl diphosphate; FPP, farnesyl diphosphate; GGPP, geranylgeranyl diphosphate; FGPP, farnesylgeranyl diphosphate.

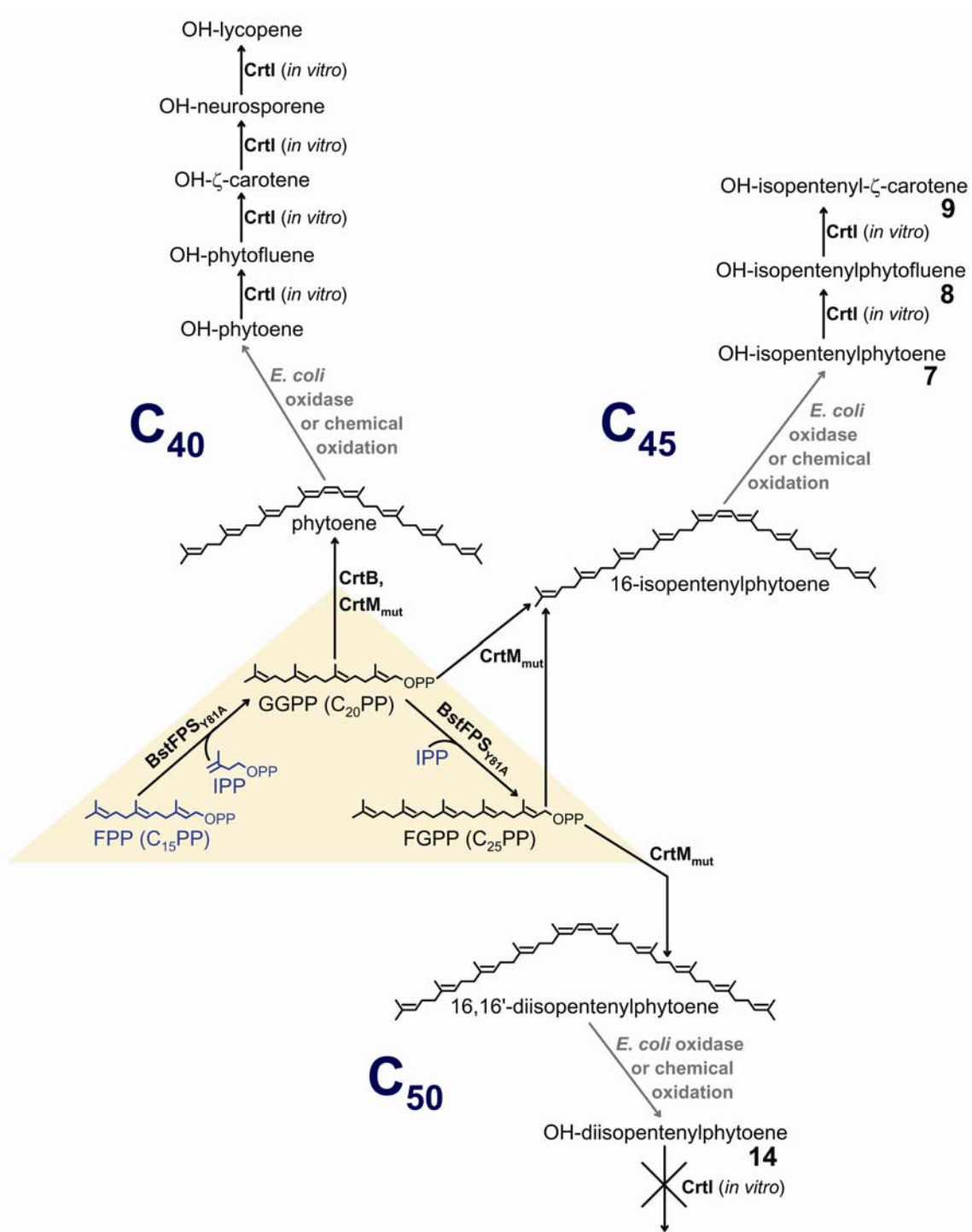


Figure 3.5

**Figure 3.5. Hydroxylation and subsequent *in vitro* desaturation of carotenoid backbones.** *E. coli* cells harboring plasmid pUCmodII-*crtM*<sub>F26L</sub>-*bstFPS*<sub>Y81A</sub> or pUCmodII-*crtM*<sub>F26A,W38A</sub>-*bstFPS*<sub>Y81A</sub> accumulate monohydroxylated phytoene as well as monohydroxylated C<sub>45</sub> and C<sub>50</sub> carotenoid backbones **7** and **14**, respectively (Figures 3.7-3.9). Neither the mechanism nor the specific sites of hydroxylation are known. *In vitro*, *E. uredoovora* CrtI catalyzes 4 desaturation steps on the hydroxylated C<sub>40</sub> backbone, with each intermediate in the desaturation sequence being detected (Table 3.3). *In vitro* desaturation of the hydroxylated C<sub>45</sub> backbone **7** yielded 1-step product **8** and 2-step product **9**. The hydroxylated C<sub>50</sub> backbone **14** was not detectably desaturated by CrtI *in vitro* (crossed-out arrow). CrtB, phytoene synthase; CrtM<sub>mut</sub>, mutant synthase CrtM<sub>F26L</sub> or CrtM<sub>F26A,W38A</sub>; IPP, isopentenyl diphosphate; FPP, farnesyl diphosphate; GGPP, geranylgeranyl diphosphate; FGPP, farnesylgeranyl diphosphate.

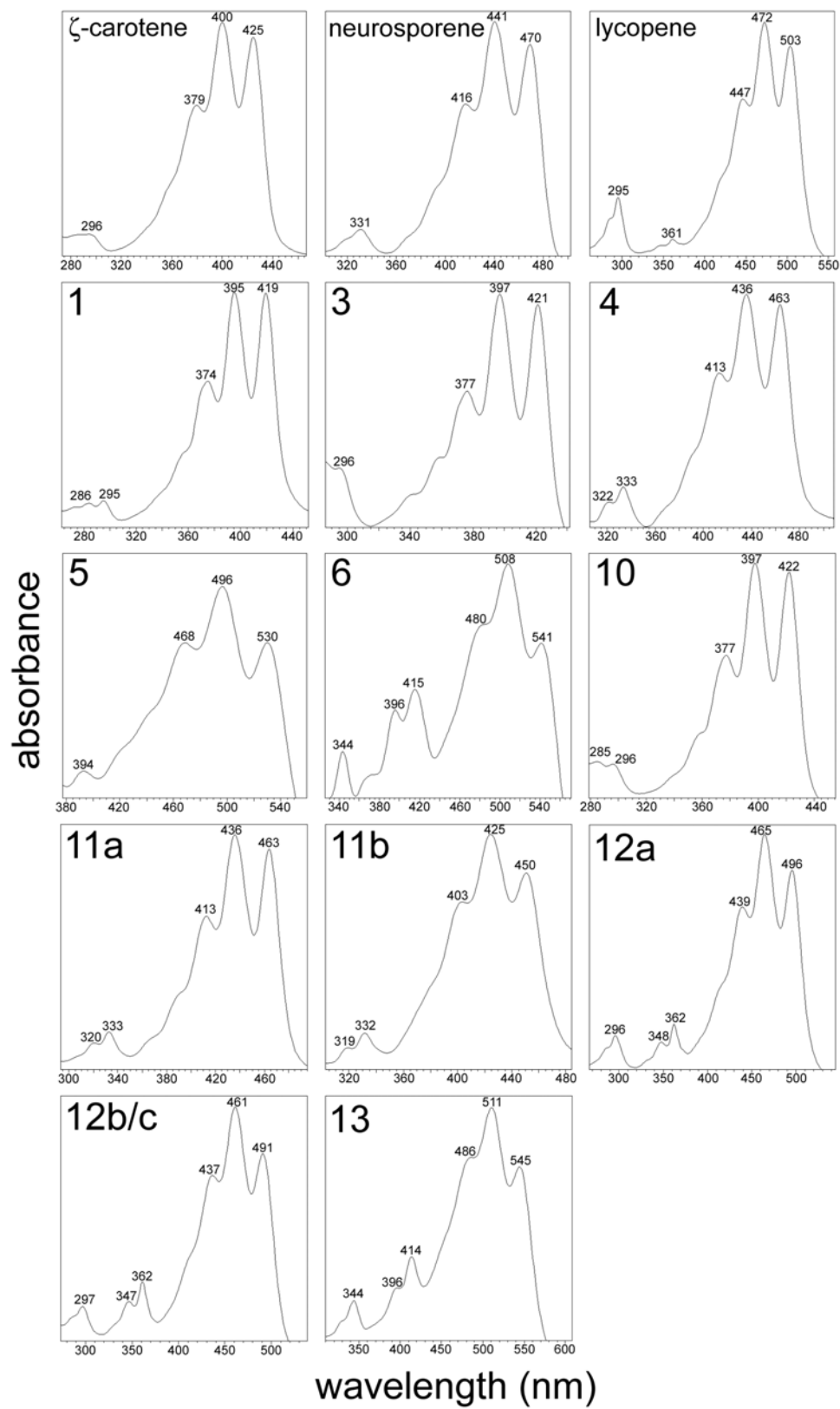
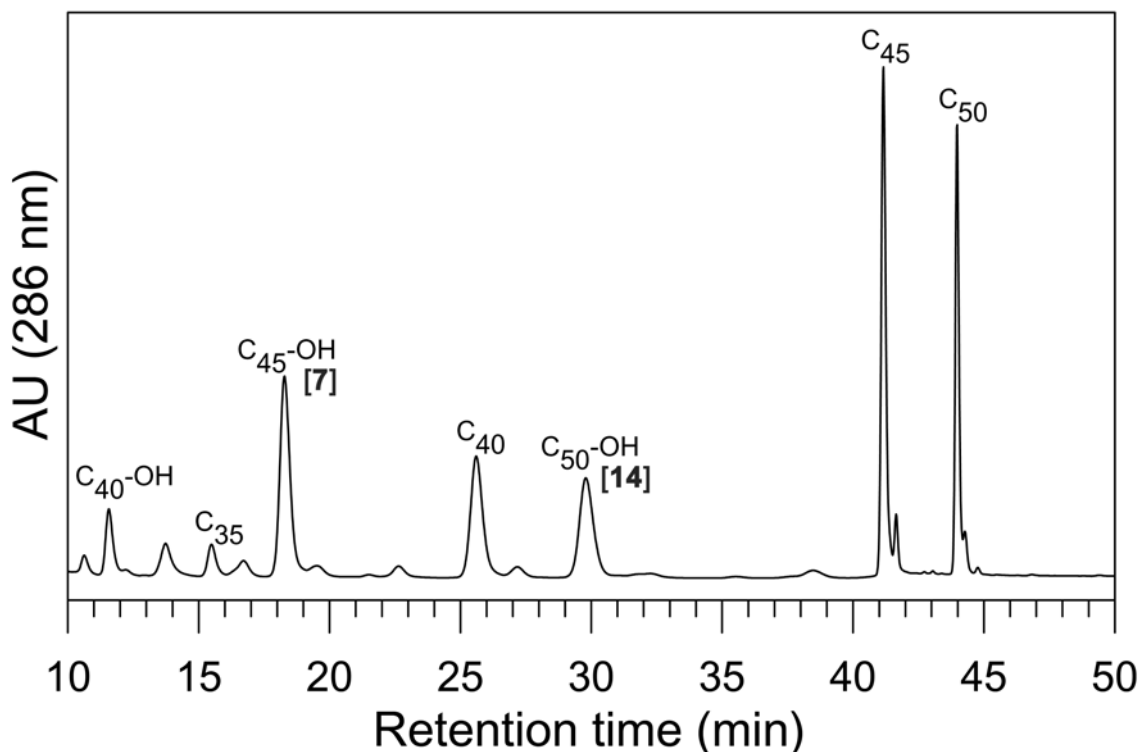
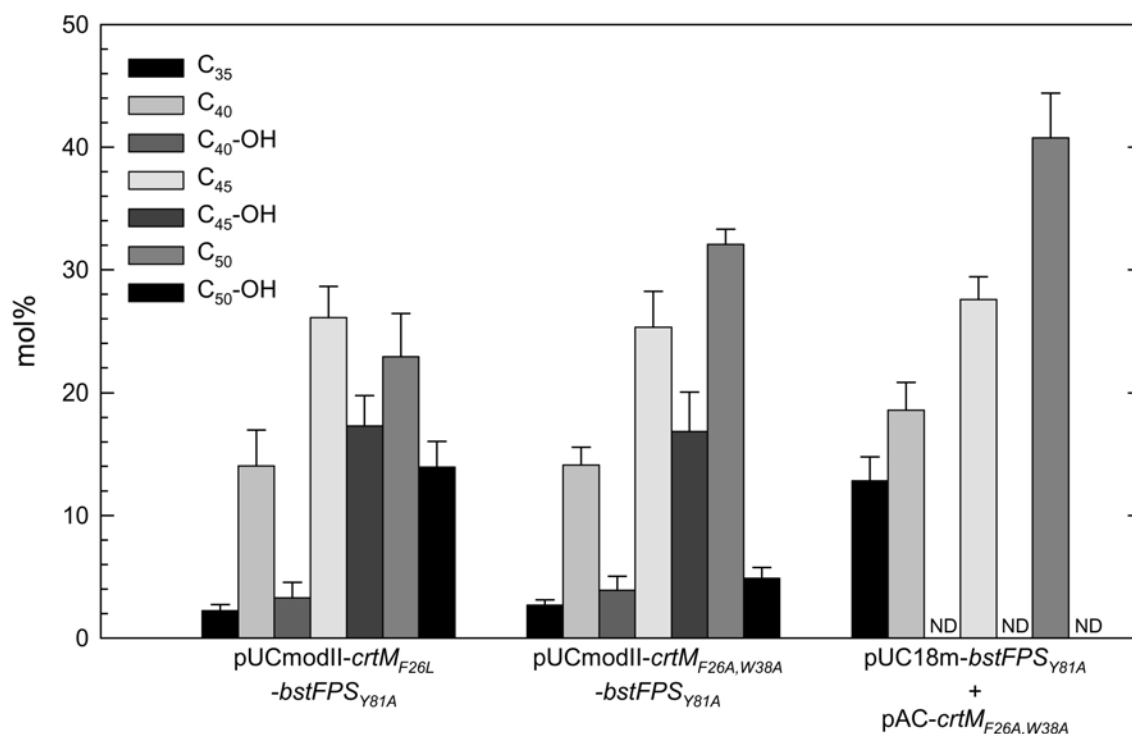


Figure 3.6

**Figure 3.6. UV-visible absorption spectra of novel carotenoids biosynthesized by recombinant *E. coli*.** Numeric labels refer to structures depicted in Figures 3.2-3.4; multiple letters indicate that the spectrum may be that of either or both structures. Spectra were measured by photodiode array directly after HPLC separation, with a mobile phase of acetonitrile:isopropanol 93:7 (by volume, see Materials and Methods). Spectra were taken before and after iodine-catalyzed photoisomerization; each spectrum shown is the most bathochromically shifted of the two. Absorption spectra of  $\zeta$ -carotene, neurosporene, and lycopene generated by *in vitro* desaturation of authentic phytoene are shown for comparison (See Figure 3.4 for structures of these C<sub>40</sub> carotenoids). Absorption maxima are labeled with the corresponding wavelength. Table 3.1 lists additional properties of these molecules; Table 3.2 lists their names.



**Figure 3.7. HPLC trace of carotenoid backbones extracted from a culture of XL1-Blue(pUCmodII-*crtM*<sub>F26L</sub>-*bstFPS*<sub>Y81A</sub>).** Carotenoids were eluted using the gradient method described in Materials and Methods. The identity of each peak was confirmed by MS; the presence of monohydroxy substituents was further confirmed by acetylation and subsequent MS (see Figure 3.9). The C<sub>40</sub> and C<sub>40</sub>-OH peaks likely represent mixtures of symmetric and asymmetric C<sub>40</sub> backbones that did not separate under these elution conditions. Labeled major peaks represent 15*Z* isomers; minor peaks eluting just after major peaks represent all-*E* isomers. Numbers in square brackets refer to products shown in Figure 3.5.



**Figure 3.8. Relative molar quantities of the carotenoid backbones produced by recombinant XL1-Blue cultures expressing BstFPS<sub>Y81A</sub> and a CrtM variant.**

Transformed plasmid(s) are shown on the horizontal axis. Bar heights represent the average of measurements of at least three independent cultures; error bars, standard deviations. Total carotenoid titers varied to a greater extent than relative molar quantities, approximate values were: pUCmodII-*crtM*<sub>F26L</sub>-*bstFPS*<sub>Y81A</sub>, ~100 nmol/g dry cells; pUCmodII-*crtM*<sub>F26A,W38A</sub>-*bstFPS*<sub>Y81A</sub>, ~300 nmol/g dry cells; pUC18m-*bstFPS*<sub>Y81A</sub> + pAC-*crtM*<sub>F26A,W38A</sub>, ~70 nmol/g dry cells. ND, not detected. The C<sub>40</sub> and C<sub>40</sub>-OH data series likely represent mixtures of symmetric and asymmetric C<sub>40</sub> backbones that did not separate by the HPLC methods described in Materials and Methods.

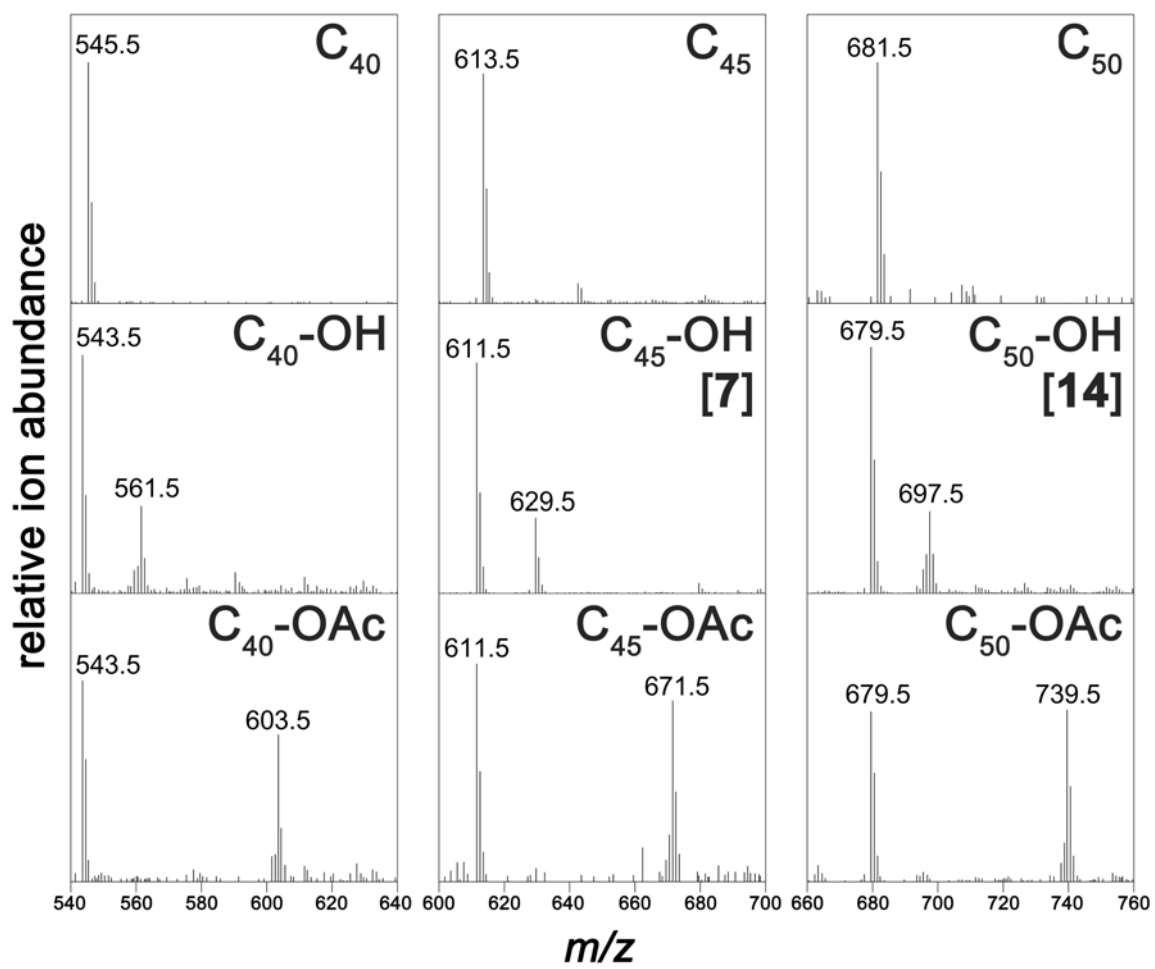
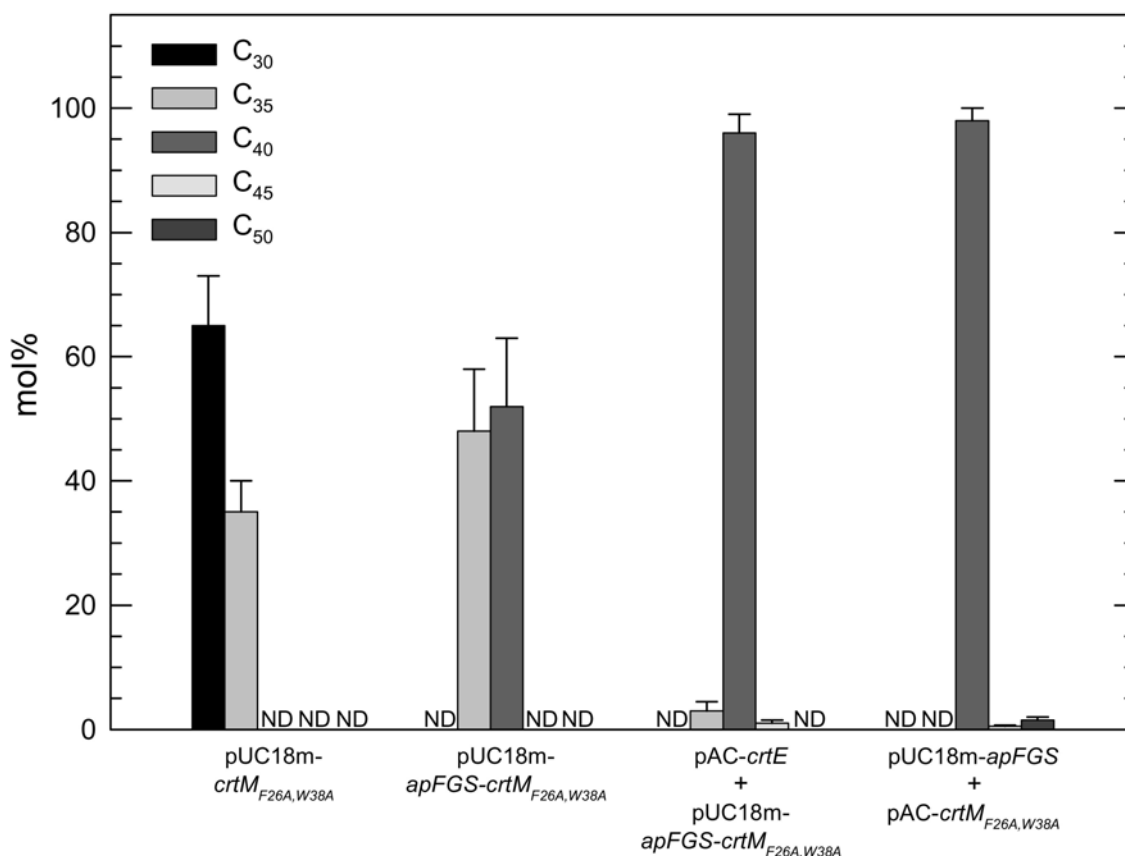


Figure 3.9

**Figure 3.9. APCI mass spectra of unmodified, hydroxylated, and acetylated carotenoid backbones.** Unmodified carotenoid backbones ionize by protonation in APCI-MS, giving  $[M+H]^+$  quasimolecular ions (calculated monoisotopic masses for carotenoid backbones: C<sub>40</sub>, 544.5 Da; C<sub>45</sub>, 612.6 Da; C<sub>50</sub>, 680.6 Da). Hydroxylated carotenoid backbones ionize by protonation followed by loss of water, yielding an  $[(M+H)-H_2O]^+$  ion ( $m/z = 543.9$  for C<sub>40</sub>-OH, 611.5 for C<sub>45</sub>-OH, and 679.5 for C<sub>50</sub>-OH) in addition to the  $[M+H]^+$  quasimolecular ion ( $m/z = 561.5$  for C<sub>40</sub>-OH, 629.5 for C<sub>45</sub>-OH, and 697.5 for C<sub>50</sub>-OH). Hydroxylated backbones were acetylated by reaction with acetic anhydride. Mass spectra of the acetylated products reveal a similar mode of ionization to their hydroxylated counterparts, yielding the  $[(M+H)-CH_3COOH]^+$  ion (identical to the  $[(M+H)-H_2O]^+$  ions listed above) in addition to the  $[M+H]^+$  quasimolecular ion ( $m/z = 603.9$  for C<sub>40</sub>-OAc, 671.5 for C<sub>45</sub>-OAc, and 739.5 for C<sub>50</sub>-OAc). Numbers in square brackets refer to products shown in Figure 3.5.



**Figure 3.10. Relative molar quantities of the carotenoid backbones produced by recombinant XL1-Blue cultures expressing ApFGS and CrtM<sub>F26A,W38A</sub>.** Transformed plasmid(s) are shown on the horizontal axis. Bar heights represent the average of measurements on two independent cultures; error bars, standard deviations. Total carotenoid titers varied to a greater extent than relative molar quantities, approximate values were: pUC18m-*crtM*<sub>F26A,W38A</sub>, ~30 nmol/g dry cells; pUC18m-*apFGS-crtM*<sub>F26A,W38A</sub>, ~100 nmol/g dry cells; pAC-*crtE* + pUC18m-*apFGS-crtM*<sub>F26A,W38A</sub>, ~300 nmol/g dry cells; pUC18m-*apFGS* + pAC-*crtM*<sub>F26A,W38A</sub>, ~100 nmol/g dry cells. ND, not detected. The relatively low proportion of C<sub>50</sub> backbones in the cultures expressing ApFGS indicates a low C<sub>25</sub>PP supply in the cells. Therefore, ApFGS acts predominantly as a C<sub>20</sub>PP synthase under these conditions, and the C<sub>40</sub> backbone population should thus consist almost exclusively of phytoene.

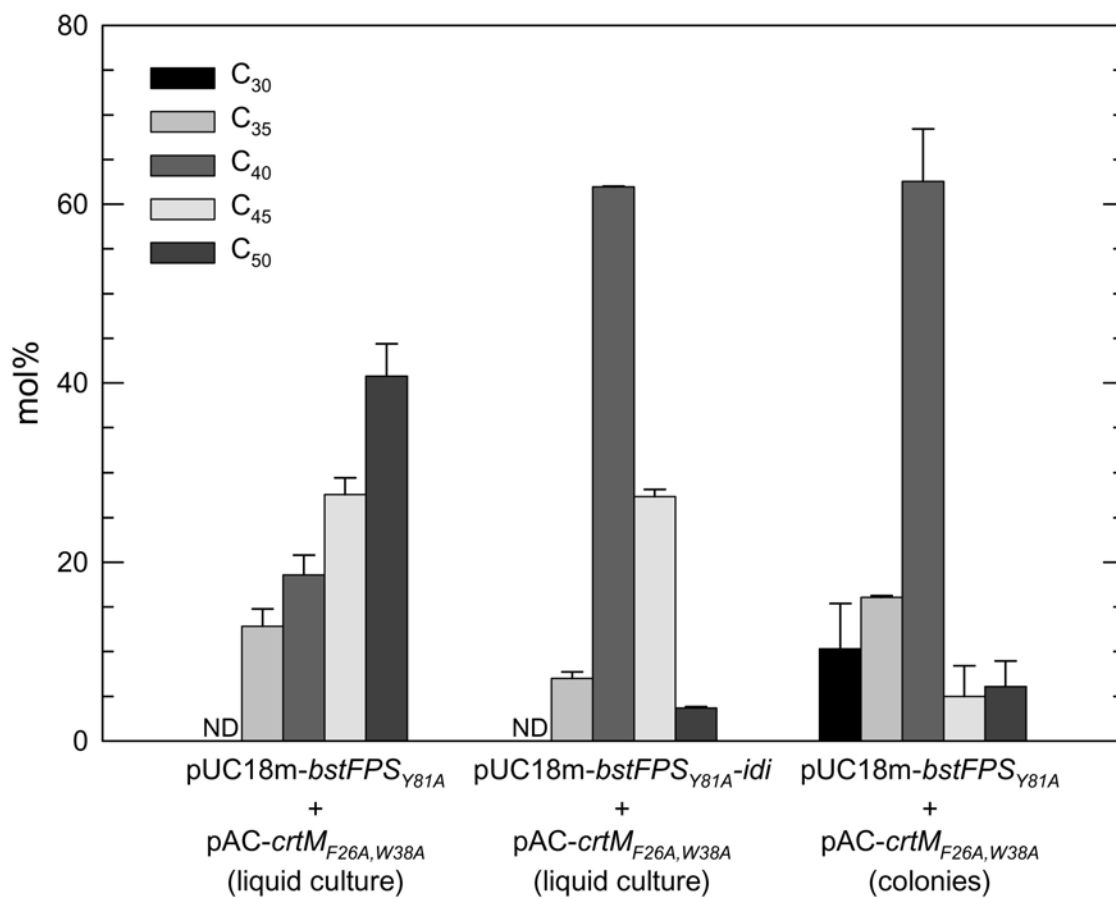


Figure 3.11

**Figure 3.11. Idi overexpression and physiological state strongly influence the distribution of carotenoid backbones in recombinant XL1-Blue cells expressing BstFPS<sub>Y81A</sub> and CrtM<sub>F26A,W38A</sub>.** Transformed plasmid(s) and physiological state (liquid culture or colonies) are shown on the horizontal axis. For the first data set, which is repeated from Figure 3.8, bar heights represent the average of measurements on four replicate cultures. For the other sets, bar heights represent the average of measurements on two independent TB liquid cultures (second set) or on collected colonies from two independent LB-agar plates (third set). Total carotenoid titers varied to a greater extent than relative molar quantities, approximate values were: pUC18m-*bstFPS*<sub>Y81A</sub> + pAC-*crtM*<sub>F26A,W38A</sub> (liquid culture), ~70 nmol/g dry cells; pUC18m-*bstFPS*<sub>Y81A-idi</sub> + pAC-*crtM*<sub>F26A,W38A</sub> (liquid culture), ~700 nmol/g dry cells; pUC18m-*bstFPS*<sub>Y81A</sub> + pAC-*crtM*<sub>F26A,W38A</sub> (colonies), ~70 nmol/g dry cells. ND, not detected. The relatively low proportion of C<sub>50</sub> backbones in the second and third data sets indicates a low C<sub>25</sub>PP supply in the cells; therefore, the C<sub>40</sub> backbone population should consist predominantly of phytoene.

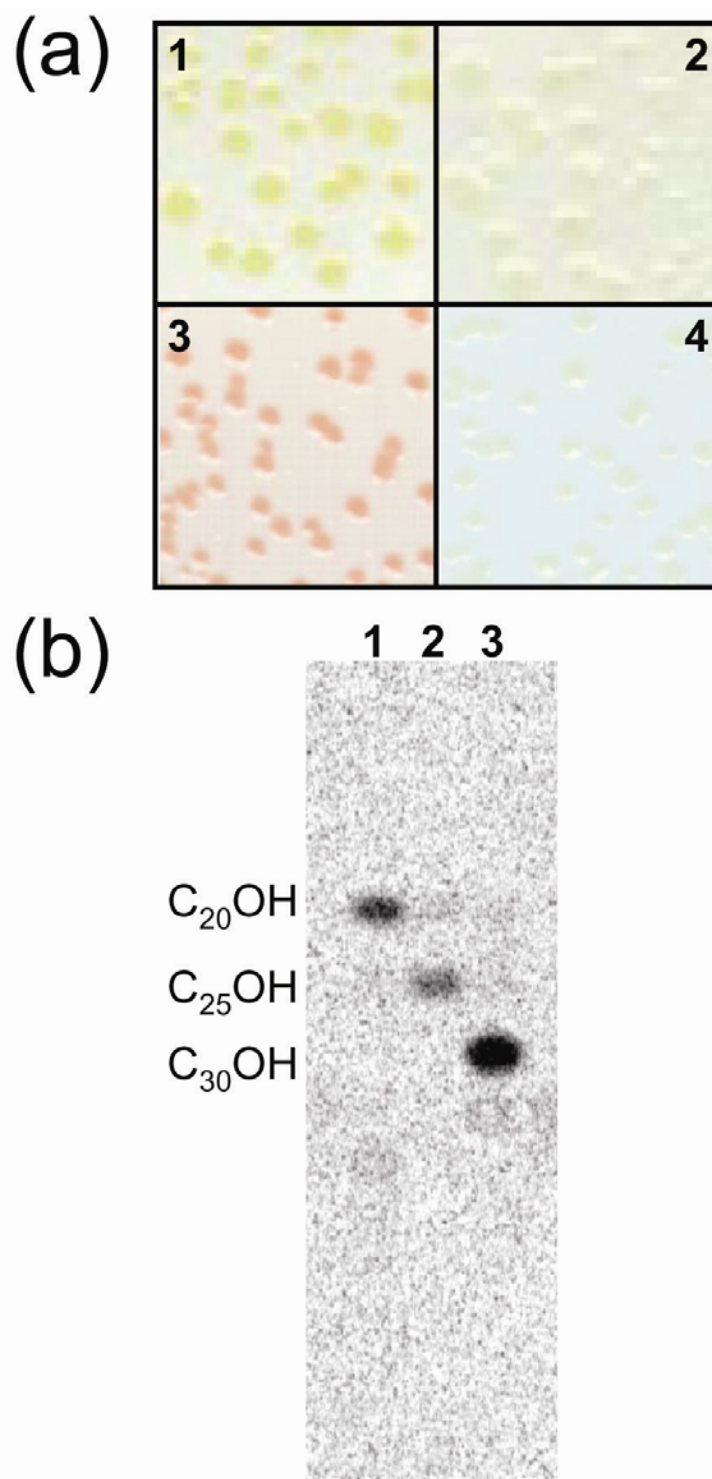


Figure 3.12

**Figure 3.12. Product specificity of *M. luteus* hexaprenyl diphosphate synthase (HexPS).** (a) Pigmentation of *E. coli* XL1-Blue colonies expressing different plasmids and imaged on white nitrocellulose: panel 1, pUC18m-*crtM-crtN*; panel 2, pUC18m-*hexPS-crtM-crtN*; panel 3, pUC18m-*crtE-crtB-crtI*; panel 4, pUC18m-*hexPS-crtB-crtI*. (b) TLC-autoradiogram of the hydrolyzed products from *in vitro* reactions of FPP ( $C_{15}PP$ ) with  $^{14}C$ -labeled IPP catalyzed by various isoprenyl diphosphate synthases: lane 1, *E. uredoovora* CrtE; lane 2, BstFPS<sub>Y81A</sub>; lane 3, HexPS. Prenyl diphosphate products were hydrolyzed with acid phosphatase to the corresponding alcohol and then separated by reverse-phase TLC (see Materials and Methods). The direction of mobile phase flow was bottom to top. This autoradiogram was obtained by Adam Hartwick.

## REFERENCES

1. **Aharoni, A., L. Gaidukov, O. Khersonsky, Q. G. S. Mc, C. Roodveldt, and D. S. Tawfik.** 2005. The 'evolvability' of promiscuous protein functions. *Nat. Genet.* **37**:73-6.
2. **Albrecht, M., G. Sandmann, D. Musker, and G. Britton.** 1991. Identification of epoxy- and hydroxyphytoene from norflurazon-treated *Scenedesmus*. *J. Agric. Food Chem.* **39**:566-569.
3. **Albrecht, M., S. Takaichi, N. Misawa, G. Schnurr, P. Böger, and G. Sandmann.** 1997. Synthesis of atypical cyclic and acyclic hydroxy carotenoids in *Escherichia coli* transformants. *J. Biotechnol.* **58**:177-185.
4. **Albrecht, M., S. Takaichi, S. Steiger, Z. Y. Wang, and G. Sandmann.** 2000. Novel hydroxycarotenoids with improved antioxidative properties produced by gene combination in *Escherichia coli*. *Nat. Biotechnol.* **18**:843-846.
5. **Aragón, C. M., F. J. Murillo, M. D. de la Guardia, and E. Cerdá-Olmedo.** 1976. An enzyme complex for the dehydrogenation of phytoene in *Phycomyces*. *Eur. J. Biochem.* **63**:71-5.
6. **Boucher, Y., M. Kamekura, and W. F. Doolittle.** 2004. Origins and evolution of isoprenoid lipid biosynthesis in archaea. *Mol. Microbiol.* **52**:515-27.
7. **Britton, G.** 1998. Overview of carotenoid biosynthesis, p. 13-147. *In* G. Britton, S. Liaaen-Jensen, and H. Pfander (ed.). *Carotenoids*, vol. 3: Biosynthesis and Metabolism. Birkhäuser Verlag, Basel.
8. **Britton, G.** 1995. Structure and properties of carotenoids in relation to function. *Faseb J.* **9**:1551-8.
9. **Britton, G.** 1995. UV/Visible Spectroscopy, p. 13-62. *In* G. Britton, S. Liaaen-Jensen, and H. Pfander (ed.). *Carotenoids*, vol. 1B: Spectroscopy. Birkhäuser Verlag, Basel.
10. **Buckingham, J.** 2004. *Dictionary of Natural Products*. Chapman & Hall/CRC Press. <http://www.chemnetbase.com/scripts/dnpweb.exe>.
11. **Burch, R. R., Y. Dong, C. Fincher, M. Goldfinger, and P. Rouviere.** 2004. Electrical properties of polyunsaturated natural products: field effect mobility of carotenoid polyenes. *Synth. Met.* **146**:43-46.
12. **Candau, R., E. R. Bejarano, and E. Cerdá-Olmedo.** 1991. *In vivo* channeling of substrates in an enzyme aggregate for beta-carotene biosynthesis. *Proc. Natl. Acad. Sci. U.S.A.* **88**:4936-40.
13. **Colodner, R.** 2005. Extended-spectrum beta-lactamases: a challenge for clinical microbiologists and infection control specialists. *Am. J. Infect. Control* **33**:104-7.
14. **Davies, B. H., C. J. Hallett, R. A. London, and A. F. Rees.** 1974. The nature of "theta-carotene." *Phytochemistry* **13**:1209-1217.
15. **Davis, J. B., L. M. Jackman, P. T. Siddons, and B. C. L. Weedon.** 1966. Carotenoids and related compounds Part XV: The structure and synthesis of phytoene, phytofluene, zeta-carotene, and neurosporene. *J. Chem. Soc. (C)*:2154-2165.

16. **De la Guardia, M. D., C. M. Aragón, F. J. Murillo, and E. Cerdá-Olmedo.** 1971. A carotenogenic enzyme aggregate in *Phycomyces*: evidence from quantitative complementation. *Proc. Natl. Acad. Sci. U.S.A.* **68**:2012-5.
17. **Edge, R., D. J. McGarvey, and T. G. Truscott.** 1997. The carotenoids as antioxidants—a review. *J. Photochem. Photobiol. B.* **41**:189-200.
18. **Englert, G.** 1995. NMR Spectroscopy, p. 147-260. *In* G. Britton, S. Liaaen-Jensen, and H. Pfander (ed.). *Carotenoids*, vol. 1B: Spectroscopy. Birkhäuser Verlag, Basel.
19. **Eugster, C. H.** 1995. Chemical Derivatization: Microscale Tests for the Presence of Common Functional Groups in Carotenoids, p. 71-80. *In* G. Britton, S. Liaaen-Jensen, and H. Pfander (ed.). *Carotenoids*, vol. 1A: Isolation and Analysis. Birkhäuser Verlag, Basel.
20. **Farmer, W. R., and J. C. Liao.** 2000. Improving lycopene production in *Escherichia coli* by engineering metabolic control. *Nat. Biotechnol.* **18**:533-537.
21. **Firn, R. D., and C. G. Jones.** 2000. The evolution of secondary metabolism—a unifying model. *Mol. Microbiol.* **37**:989-994.
22. **Firn, R. D., and C. G. Jones.** 1996. An explanation of secondary product "redundancy," p. 295-312. *In* J. T. Romeo, J. A. Saunders, and P. Barbosa (ed.), *Recent Advances in Phytochemistry*, vol. 30. *Phytochemical Diversity and Redundancy in Ecological Interactions*. Plenum Press, New York.
23. **Firn, R. D., and C. G. Jones.** 2003. Natural products—a simple model to explain chemical diversity. *Nat. Prod. Rep.* **20**:382-391.
24. **Fraser, P. D., N. Misawa, H. Linden, S. Yamano, K. Kobayashi, and G. Sandmann.** 1992. Expression in *Escherichia coli*, purification, and reactivation of the recombinant *Erwinia uredovora* phytoene desaturase. *J. Biol. Chem.* **267**:19891-19895.
25. **Hausmann, A., and G. Sandmann.** 2000. A single five-step desaturase is involved in the carotenoid biosynthesis pathway to beta-carotene and torulene in *Neurospora crassa*. *Fungal Genetics and Biology* **30**:147-153.
26. **Hemmi, H., S. Ikejiri, S. Yamashita, and T. Nishino.** 2002. Novel medium-chain prenyl diphosphate synthase from the thermoacidophilic archaeon *Sulfolobus solfataricus*. *J. Bacteriol.* **184**:615-20.
27. **Jensen, R. A.** 1976. Enzyme recruitment in evolution of new function. *Annu. Rev. Microbiol.* **30**:409-25.
28. **Jones, C. G., and R. D. Firn.** 1991. On the evolution of plant secondary chemical diversity. *Philos. Trans. R. Soc. Lond. Ser. B-Biol. Sci.* **333**:273-280.
29. **Karrer, P., and C. H. Eugster.** 1951. Carotinoidsynthesen 8. Synthese des dodecapreno-beta-carotins. *Helv. Chim. Acta* **34**:1805-1814.
30. **Krubasik, P., M. Kobayashi, and G. Sandmann.** 2001. Expression and functional analysis of a gene cluster involved in the synthesis of decaprenoxanthin reveals the mechanisms for C<sub>50</sub> carotenoid formation. *Eur. J. Biochem.* **268**:3702-3708.
31. **Lee, P. C., A. Z. R. Momen, B. N. Mijts, and C. Schmidt-Dannert.** 2003. Biosynthesis of structurally novel carotenoids in *Escherichia coli*. *Chem. Biol.* **10**:453-462.

32. **Liaaen-Jensen, S.** 1995. Combined Approach: Identification and Structure Elucidation of Carotenoids, p. 343-354. *In* G. Britton, S. Liaaen-Jensen, and H. Pfander (ed.). Carotenoids, vol. 1B: Spectroscopy. Birkhäuser Verlag, Basel.
33. **Linden, H., N. Misawa, D. Chamovitz, I. Pecker, J. Hirschberg, and G. Sandmann.** 1991. Functional complementation in *Escherichia coli* of different phytoene desaturase genes and analysis of accumulated carotenes. *Z. Naturforsch. (C)* **46**:1045-1051.
34. **Lorenz, R. T., and G. R. Cysewski.** 2000. Commercial potential for *Haematococcus* microalgae as a natural source of astaxanthin. *Trends Biotechnol.* **18**:160-7.
35. **Mijts, B. N., P. C. Lee, and C. Schmidt-Dannert.** 2005. Identification of a carotenoid oxygenase synthesizing acyclic xanthophylls: combinatorial biosynthesis and directed evolution. *Chem. Biol.* **12**:453-60.
36. **Murillo, F. J., S. Torres-Martinez, C. M. Aragón, and E. Cerdá-Olmedo.** 1981. Substrate transfer in carotene biosynthesis in *Phycomyces*. *Eur. J. Biochem.* **119**:511-6.
37. **Ohnuma, S., K. Narita, T. Nakazawa, C. Ishida, Y. Takeuchi, C. Ohto, and T. Nishino.** 1996. A role of the amino acid residue located on the fifth position before the first aspartate-rich motif of farnesyl diphosphate synthase on determination of the final product. *J. Biol. Chem.* **271**:30748-30754.
38. **Ohnuma, S. I., T. Nakazawa, H. Hemmi, A. M. Hallberg, T. Koyama, K. Ogura, and T. Nishino.** 1996. Conversion from farnesyl diphosphate synthase to geranylgeranyl diphosphate synthase by random chemical mutagenesis. *J. Biol. Chem.* **271**:10087-10095.
39. **Raisig, A., G. Bartley, P. Scolnik, and G. Sandmann.** 1996. Purification in an active state and properties of the 3-step phytoene desaturase from *Rhodobacter capsulatus* overexpressed in *Escherichia coli*. *J. Biochem. (Tokyo)* **119**:559-64.
40. **Raisig, A., and G. Sandmann.** 2001. Functional properties of diapophytoene and related desaturases of C<sub>30</sub> and C<sub>40</sub> carotenoid biosynthetic pathways. *Biochim. Biophys. Acta Mol. Cell Biol. Lipids* **1533**:164-170.
41. **Rison, S. C., and J. M. Thornton.** 2002. Pathway evolution, structurally speaking. *Curr. Opin. Struct. Biol.* **12**:374-82.
42. **Sandmann, G.** 2002. Combinatorial biosynthesis of carotenoids in a heterologous host: A powerful approach for the biosynthesis of novel structures. *ChemBioChem* **3**:629-635.
43. **Sandmann, G., M. Albrecht, G. Schnurr, O. Knorzer, and P. Boger.** 1999. The biotechnological potential and design of novel carotenoids by gene combination in *Escherichia coli*. *Trends Biotechnol.* **17**:233-237.
44. **Schiedt, K., and S. Liaaen-Jensen.** 1995. Isolation and Analysis, p. 81-108. *In* G. Britton, S. Liaaen-Jensen, and H. Pfander (ed.). Carotenoids, vol. 1A: Isolation and Analysis. Birkhäuser Verlag, Basel.
45. **Schmidt-Dannert, C.** 2000. Engineering novel carotenoids in microorganisms. *Curr. Opin. Biotechnol.* **11**:255-261.
46. **Schmidt-Dannert, C., D. Umeno, and F. H. Arnold.** 2000. Molecular breeding of carotenoid biosynthetic pathways. *Nat. Biotechnol.* **18**:750-753.

47. **Shimizu, N., T. Koyama, and K. Ogura.** 1998. Molecular cloning, expression, and characterization of the genes encoding the two essential protein components of *Micrococcus luteus* B-P 26 hexaprenyl diphosphate synthase. *J. Bacteriol.* **180**:1578-81.
48. **Steiger, S., S. Takaichi, and G. Sandmann.** 2002. Heterologous production of two unusual acyclic carotenoids, 1,1'-dihydroxy-3,4-didehydrolycopene and 1-hydroxy-3,4,3',4'-tetrahydrolycopene by combination of the *crtC* and *crtD* genes from *Rhodobacter* and *Rubrivivax*. *J. Biotechnol.* **97**:51-8.
49. **Tachibana, A.** 1994. A novel prenyltransferase, farnesylgeranyl diphosphate synthase, from the haloalkaliphilic archaeon, *Natronobacterium pharaonis*. *FEBS Lett.* **341**:291-4.
50. **Tachibana, A., Y. Yano, S. Otani, N. Nomura, Y. Sako, and M. Taniguchi.** 2000. Novel prenyltransferase gene encoding farnesylgeranyl diphosphate synthase from a hyperthermophilic archaeon, *Aeropyrum pernix*: Molecular evolution with alteration in product specificity. *Eur. J. Biochem.* **267**:321-8.
51. **Takaichi, S.** 2000. Characterization of carotenes in a combination of a C<sub>18</sub> HPLC column with isocratic elution and absorption spectra with a photodiode-array detector. *Photosynth. Res.* **65**:93-99.
52. **Tao, L., A. Schenzle, J. M. Odom, and Q. Cheng.** 2005. Novel carotenoid oxidase involved in biosynthesis of 4,4'-diapolyycopene dialdehyde. *Appl. Environ. Microbiol.* **71**:3294-301.
53. **Umeno, D., and F. H. Arnold.** 2003. A C<sub>35</sub> carotenoid biosynthetic pathway. *Appl. Environ. Microbiol.* **69**:3573-3579.
54. **Umeno, D., and F. H. Arnold.** 2004. Evolution of a pathway to novel long-chain carotenoids. *J. Bacteriol.* **186**:1531-1536.
55. **Umeno, D., K. Hiraga, and F. H. Arnold.** 2003. Method to protect a targeted amino acid residue during random mutagenesis. *Nucleic Acids Res.* **31**:e91.
56. **Umeno, D., A. V. Tobias, and F. H. Arnold.** 2002. Evolution of the C<sub>30</sub> carotenoid synthase CrtM for function in a C<sub>40</sub> pathway. *J. Bacteriol.* **184**:6690-6699.
57. **Vershinin, A.** 1999. Biological functions of carotenoids—diversity and evolution. *Biofactors* **10**:99-104.
58. **Wang, C. W., and J. C. Liao.** 2001. Alteration of product specificity of *Rhodobacter sphaeroides* phytoene desaturase by directed evolution. *J. Biol. Chem.* **276**:41161-41164.
59. **Wang, C. W., M. K. Oh, and J. C. Liao.** 1999. Engineered isoprenoid pathway enhances astaxanthin production in *Escherichia coli*. *Biotechnol. Bioeng.* **62**:235-241.
60. **Wang, K., and S. Ohnuma.** 1999. Chain-length determination mechanism of isoprenyl diphosphate synthases and implications for molecular evolution. *Trends Biochem. Sci.* **24**:445-451.
61. **Woodall, A. A., S. W. M. Lee, R. J. Weesie, M. J. Jackson, and G. Britton.** 1997. Oxidation of carotenoids by free radicals: relationship between structure and reactivity. *Biochim. Biophys. Acta-Gen. Subj.* **1336**:33-42.
62. **Ycas, M.** 1974. On earlier states of the biochemical system. *J. Theor. Biol.* **44**:145-60.

63. **Young, A. J., and G. M. Lowe.** 2001. Antioxidant and prooxidant properties of carotenoids. *Arch. Biochem. Biophys.* **385**:20-7.
64. **Zechmeister, L., and B. K. Koe.** 1954. Stepwise dehydrogenation of the colorless polyenes phytoene and phytofluene with N-bromosuccinimide to carotenoid pigments. *J. Am. Chem. Soc.* **76**:2923-2926.